

# Systemic Risk from Overlapping Portfolios: A Multi-Objective Optimization Framework

Alessandro Sulas<sup>a</sup>      Dietmar Maringer<sup>b</sup>  
Sandra Paterlini<sup>a</sup>

<sup>a</sup>Department of Economics and Management, University of Trento

<sup>b</sup> Faculty of Economics and Business, University of Basel

This version: April 30, 2024

## Abstract

We present a multi-objective portfolio optimization framework to minimize systemic risk arising from overlapping portfolios while accounting for individual risk. To address non-convexity in systemic risk, we introduce an Evolutionary Search algorithm that enables efficient exploration of the solution space. Applying our framework to EBA data, we find that minimizing systemic risk results in highly concentrated and diverse portfolios, adding empirical evidence to a growing literature on the ambiguous effects of diversification on systemic risk. In contrast, individual risk-optimal allocations exhibit high portfolio diversification and homogeneity. By characterizing a set of efficient frontiers, we identify a trade-off between individual and social optimality. Even a small preference for minimizing systemic risk leads to optimal portfolios on the frontier that differ significantly from the observed ones, suggesting potential inefficiencies in current portfolio structures.

*Keywords:* Asset Allocation Diversification Networks Fire sales Evolutionary Search

*JEL Codes:* G01 C61 G11 G20

# 1 Introduction

Interconnectedness have been recognised as a significant source of fragility for the financial system over the past decade (Yellen, 2013). Since the first studies (Allen and Gale, 2000; Freixas et al., 2000) there has been a broad consensus on its role as a channel for transmitting shocks to the system, besides providing opportunities for risk sharing. For this reason, especially in the aftermath of the Great Financial Crisis, much research has been devoted to identifying the main structural determinants of systemic risk and to studying the potential trade-offs between robustness and fragility of different connectivity patterns (Gai and Kapadia, 2010; Elliott et al., 2014; Acemoglu et al., 2015). Connections between financial institutions are nowadays naturally modeled in network settings, which can comprise different types of links, ranging from direct financing contracts to information networks (Benoit et al., 2017). For this reason, an increasing number of studies adopts multi-layer network frameworks. Among the layers that can give rise to financial contagion between institutions, direct financing contracts are the most widely studied. However, contagion can also be driven by asset sales through price-mediated spillovers (Cifuentes et al., 2005), which create indirect linkages between institutions that add to direct financing relationships, and increase the potential for shock transmission. Empirical evidence shows that indirect linkages are also relevant between different types of institutions (Barucca et al., 2021), involve different types of financial instruments (Falato et al., 2021), and are also significant at the international level between different financial systems (Giudici et al., 2020), both as individual drivers of systemic losses in fire-sale scenarios (Ellul et al., 2011; Shleifer and Vishny, 2011) and in their interaction with direct linkages (Caccioli et al., 2015; Poledna et al., 2015; Glasserman and Young, 2015). Therefore, providing general results on how asset allocation contributes to determining the fragility of the system is essential to gain a complete picture of potential sources of instability in the financial system and develop appropriate risk monitoring and mitigation tools. For this reason, some contributions have begun to study ways to model links between institutions resulting from portfolio overlaps and develop appropriate measures of systemic risk (Greenwood et al., 2015; Cont and Schaanning, 2019; Duarte and Eisenbach, 2021; Poledna et al., 2021; Cao et al., 2021). Despite significant advances in measurement and monitoring, there has been limited research on the relationship between alternative portfolio allocation structures and systemic risk. In particular, it remains unclear whether the fragility drivers suggested by the literature for direct interbank exposures also apply to indirect linkages. In this respect, growing research suggests a potential detrimental effect of diversification for financial stability. While individual risk minimization would drive portfolios towards more diversified allocations, some theoretical studies

find that financial institutions, by diversifying their portfolios in order to reduce their exposure to idiosyncratic shocks, end up holding very similar and highly correlated portfolios. By doing so, they expose themselves to common shocks, thus increasing the probability of massive defaults (Acharya, 2009; Wagner, 2010; Ibragimov et al., 2011). In particular, Wagner (2010) and Ibragimov et al. (2011) find that above a certain level, diversification can become excessive, highlighting a trade-off between individually and socially optimal diversification, as also stressed in Beale et al. (2011). These works define systemic risk in terms of probability of joint failure of many financial institutions due to exposure to common systematic shocks. In portfolio overlap models, systemic risk is endogenously determined by the structure of asset allocation, giving rise to indirect connections between financial institutions. These connections, while in normal times are a natural by-product of risk sharing, can become channels for the transmission of idiosyncratic shocks in interaction with leverage (Greenwood et al., 2015). While the role of diversification as a source of fragility in case of systematic shocks has so far received large attention<sup>1</sup>, its role in creating shock transmission channels has been much less studied. Simulations conducted by Caccioli et al. (2014) suggest a non-monotonic relationship between diversification and probability of contagion, finding two phase-transitions in the relationship. Very low and very high levels of diversification are found to be associated with relatively low probabilities of contagion, while intermediate levels are associated with the highest contagion probability. However, they also find that when contagion does occur, it involves an increasing number of institutions for higher levels of diversification. These insights on the diversification-systemic risk relationship raise the issue of how portfolio allocations should be structured in order to minimize systemic risk. Capponi and Weber (2024) develop a model of systemic diversification, as opposed to independent individual diversification, where banks accounting for fire-sales externalities end up holding diverse portfolios to reduce the probability and magnitude of fire sales events. Adopting a social planner perspective, Awiszus et al. (2022), find that depending on financial institutions' systemicness and assets' shock distribution, socially optimal portfolio allocation can deviate substantially from perfect diversification.

The potential ambiguity of diversification raises concerns about the safety implications of actual portfolio allocations by financial institutions. Efforts to increase diversification may unintentionally compromise financial stability while attempting to strengthen the safety of individual institutions. At the same time, low levels of diversification might nevertheless be inefficient from a systemic perspective, and a path to safer allocation may exist that also avoids deterioration in individual risk

---

<sup>1</sup>See Jackson and Pernoud (2021) for a recent review of the literature.

exposures. Recent works have started to apply constrained optimization problems to financial networks to determine the asset rebalancing needed to make financial systems safer from a systemic perspective. Diem et al. (2020) and Krause et al. (2021) optimize direct networks by reallocating interbank claims from observed data and find that systemically risk-optimal structures are significantly sparser than observed. Even with individual indifference constraints that account for potential trade-offs with individual risk, they find room for improvement in the systemic risk dimension. Pichler et al. (2021) apply the same approach to a portfolio overlap network. In particular, they find portfolio allocations that minimize systemic risk under size and individual risk-return constraints, such that more resilient structures can be achieved through optimal portfolio rebalancing. Efficient asset allocations are found to be comparable to the status quo in terms of aggregate measures of portfolio diversification and the resulting network topology. These results, which highlight the potential for reducing systemic risk while still preserving individual preferences, raise some questions about the options available to a regulator seeking efficient combinations of individual and social optimality. Portfolio rebalancing could be costly and may require significant intervention to reach optimal configurations. A crucial aspect to consider is how close we are to optimal structures and how much weight should be given to individual and social optimality in the decision-making process. In addition, systemic risk in portfolio overlap models has so far focused on the consequences of asset sales in terms of downward pressure on the assets affected by the sales. Although limited, there is evidence of spillovers between asset prices (Greenwood, 2005), so that the extent of contagion could be broader.

In this paper, we address these issues by studying optimal asset allocations with respect to systemic risk from a portfolio overlap perspective. To account for the trade-off between individual and systemic optimality, we investigate efficient allocations by developing a multi-objective optimization framework based on a weighted objective function that includes both individual and systemic risk components. We measure individual and systemic risk using aggregate, system-level functions and find optimal structures over a wide range of preferences for the two components controlled by a single parameter, thereby characterizing an efficient individual-systemic risk frontier. To assess potential differences in measured systemic risk, we provide results for both a standard portfolio overlap model and an extended model that incorporates cross-sectional asset price spillovers. The optimization problem we formulate poses significant analytical challenges. Since systemic risk arises from the joint distribution of individual exposures, aggregated as a matrix of interacting portfolio allocations, such a problem is analytically intractable except for very small systems and under oversimplifying assumptions. Moreover, due to the non-convex behavior of systemic risk with respect to the choice variables, standard solvers are of-

ten unable to reach the global optimum. To overcome these problems, we introduce a novel heuristic Evolutionary Search optimization algorithm that offers flexibility in the definition of the objective function and applicability to a wide range of settings.

We apply our optimization framework and the proposed algorithm to the sovereign portfolios of a sample of European banks and highlight the existence of a trade off between the systemic and individual dimension. On one hand, optimal structures from a pure systemic risk perspective are characterized by a higher degree of portfolio concentration and a higher level of individual exposure to market risk. On the other hand, optimizing for aggregate individual risk leads to highly diversified allocations that also have a high degree of systemic risk. By varying the degree of preference for individual risk in a multi-objective setting, we characterize a data-driven Pareto frontier between the two risk components and identify the main features of the financial system on the frontier. Even when systemic risk is given a small weight in the objective function, optimal structures differ substantially from the observed data, suggesting both systemic and individual risk inefficiencies in status quo portfolio allocations. By introducing cross-sectional spillovers, we show that although the macro-structural features of optimal allocations are not significantly altered, systemic risk is amplified by the positive dependence structure between the considered assets and may be underestimated for the European case. Our results offer several points of interest for both policy and research. First, we provide a valuable method for assessing the state of the system in terms of its distance from an efficient combination of individual and systemic risk. Based on a single parameter, we are able to span the entire Pareto frontier of efficient portfolios, which could be a useful reference for guiding optimal allocations based on a relative systemic-individual risk appetite in a multi-criteria decision making (MCDM) framework. Second, we provide new empirical evidence on the effect of diversification on systemic risk from portfolio overlap for a relevant context. Maximally diversified portfolios are associated with high systemic risk, while minimal systemic risk portfolios show a degree of concentration consistent with the observed data. However, similar overall levels of diversification can mask very different levels of systemic risk. Diversification toward more liquid assets leads to much more resilient structures, while at the systemic risk optimum, less liquid assets tend to be “isolated” in the fewest number of portfolios.

Overall, with this paper we contribute to a better understanding of the relationship between systemic risk and the structure of the financial system. The tension between the benefits of diversification in terms of individual risk and its potential systemic costs can provide a rationale for some degree of portfolio concentration. Furthermore, we offer a methodological contribution, presenting a robust algorithm for solving non-convex constrained matrix optimizations, that exhibits remarkable flexibility, efficiency, and ability to escape local optima.

The remainder of the paper is organized as follows. In Section 2, we introduce a general portfolio overlap model for a banking system and define the optimization framework. In Section 3, we present the data, objective functions, and optimization strategy. In Section 4, we provide analytical insights into the objective functions and the optimal solutions. In Section 5 we present the results of the optimization applied to European banks and comment on them in Section 6. Section 7 concludes.

## 2 General setting

### 2.1 A model of portfolio overlap networks

We consider a financial system comprising  $N$  financial institutions (hereafter, banks), each investing in a portfolio of  $K$  marked-to-market assets, having multivariate normal returns with mean  $\mathbf{0}$  and covariance matrix  $\Sigma$ .<sup>2</sup> Denoting by  $x_{ik}$  the amount invested by bank  $i$  in asset  $k$ , the set of portfolios is described by the  $N \times K$  matrix  $\mathbf{X} = \{x_{ik}\}$ . All events in the system occur at time  $t$ , with variables implicitly defined at that time. In this system, connections between banks are established through asset sales that cause price movements<sup>3</sup>, which are reflected in mark-to-market losses in the portfolios of banks holding the same assets. Asset sales can be triggered by deleveraging decisions following shocks to external assets (i.e., not included in the trading book), as modeled in Greenwood et al. (2015) and Poledna et al. (2021). Regardless of the reason for deleveraging and the amount of sales needed to restore the required level of leverage, we model these linkages using a standard portfolio overlap framework inspired by Greenwood et al. (2015) and Cont and Schaanning (2017). Specifically, we assume that the percentage price impact for asset  $k$  resulting from quantity  $q_k$  sold in the market can be expressed as a linear function of the quantity sold:

$$\Delta p_k(q_k) = \gamma_k q_k \quad (1)$$

where  $\gamma_k$  is the linear price impact parameter for asset  $k$ , and  $q_k$  is the quantity sold in the market in the reference period.<sup>4</sup> This setting allows modelling the connection between banks  $i$  and  $j$  — i.e., their total portfolio overlap — as the maximum

---

<sup>2</sup>The assumption of normality is not essential at this stage of the model, but we introduce it since it simplifies formulas for individual risk measures. As for the mean zero assumption, we introduce it since it is consistent with the observed data on sovereign indices. Nevertheless, extensions for different expected returns assumptions are possible.

<sup>3</sup>We implicitly assume that the fundamental value of the asset is unchanged, and the resulting price variation depends on a temporary adjustment due to excess order flows (Chernenko and Sunderam, 2020) resulting from exogenous portfolio adjustment decisions.

<sup>4</sup>At this stage, for simplicity, since all events take place in  $t$ , we consider a liquidation period of one trading day. We also implicitly assume that the value of  $\gamma_k$  is such that  $\Delta p_k \in (0, 1)$  for  $q_k > 0$ , i.e., the market liquidity is sufficient to prevent the sales from driving the prices to 0.

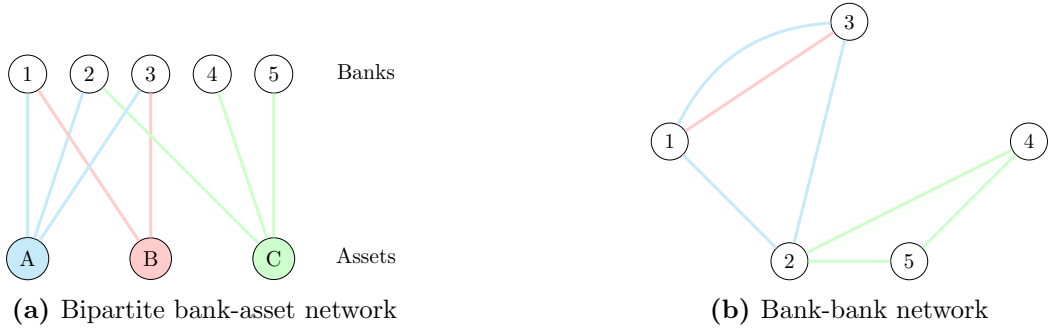


**Figure 1:** Portfolio overlap network. Panel (a) shows a bipartite network representation of a system with 5 banks investing in 3 assets, where a link is drawn between a bank and an asset if the bank holds the asset. Panel (b) shows the resulting bank-bank network, where a link is drawn between two banks for each common asset in their portfolios.

potential fire-sale loss that bank  $i$  can cause to bank  $j$  by liquidating its entire portfolio:

$$w_{ij}^{aff} = \sum_{k=1}^K x_{ik} \gamma_k x_{jk} \quad (2)$$

where the superscript refers to the fact that links are created by price effects only on assets affected by sales. In network theory terms, the set of banks' asset investments is a weighted bipartite network, where an edge between bank  $i$  and asset  $k$  is established if  $x_{ik} > 0$ , and the amount  $x_{ik}$  is the weight of the edge. Equation (2) defines the one-mode projection (Newman, 2018; Jackson, 2008) of the bipartite network expressed by the matrix  $\mathbf{X}$ , which is represented by the weighted adjacency matrix  $\mathbf{W}^{aff} = \{w_{ij}^{aff}\}$ . A stylized representation of the network is reported in Figure 1.

The formula in (2) only considers links between banks  $i$  and  $j$  due to potential effects on the prices of the assets affected by the sales. However, the sale of an asset  $k$  may not only have an effect on the asset  $k$  itself, but may also generate spillovers to the prices of assets not affected by the sales due to adjustments in arbitrageurs' portfolios (Greenwood, 2005). To account for this additional source of contagion, an extended price impact formula must be introduced. We assume that a change in the price of the security  $k$  is transmitted to a change in the price of the security  $l$  through a coefficient  $\beta_{lk}$  such that:

$$\Delta p_l(\Delta p_k) = \beta_{lk} \Delta p_k \quad (3)$$

where  $\Delta p_l(\Delta p_k)$  is the change in the price of asset  $l$  resulting from a change in the price of asset  $k$ . The existence and magnitude of such spillovers depend on the conditional distribution of asset returns and the dynamics observed in asset markets during a fire-sale event. In the next section, we propose a simple method for estimating such spillovers that can take into account the sparsity of the dependence

structure and the correlations arising from exposure to common factors. Leaving aside the estimation of spillovers, and assuming a conditional dependence structure expressed by coefficients  $\beta_{lk}$ , our banking system can thus be described by an extended network of portfolio overlaps, defined as the set of links  $w_{ij}^{tot}$  such that:

$$w_{ij}^{tot} = \sum_{k=1}^K x_{ik} \gamma_k \beta_{lk} x_{jl} \quad (4)$$

that can be decomposed into a part due to the price impact on the affected asset, expressed by (2), and a part of the price impact deriving from spillovers, which adds the information contained in the  $\beta_{lk}$  coefficients:

$$w_{ij}^{tot} = w_{ij}^{aff} + w_{ij}^{unaff} = \sum_{k=1}^K x_{ik} \gamma_k x_{jk} + \sum_{k=1}^K \sum_{l \neq k} x_{ik} \gamma_k \beta_{lk} x_{jl} \quad (5)$$

where  $w_{ij}^{aff}$  measures the link created by potential contagion through price effects on assets affected by fire sales, while  $w_{ij}^{unaff}$  measures contagion through spillover to prices of assets not affected by sales. This second term can be an additional source of risk when assets have a positive dependence structure, while in the case of independent asset classes (5) would coincide with (2). Based on the matrix of portfolios  $\mathbf{X}$ , we can represent the extended portfolio overlap network with the adjacency matrix:

$$\mathbf{W}^{tot} = \mathbf{X} \mathbf{\Gamma} \mathbf{B}' \mathbf{X}' \quad (6)$$

where  $\mathbf{\Gamma}$  is a  $K \times K$  diagonal matrix of price impact coefficients  $\gamma_k$ ,  $\mathbf{B} = \{\beta_{kl}\}$  is a  $K \times K$  having  $\beta_{kl} = 1$  for diagonal elements  $k = l$ . Under no-spillover assumption, the matrix  $\mathbf{B}$  coincides with the identity matrix  $\mathbf{I}_K$ , and the network can be expressed as:

$$\mathbf{W}^{aff} = \mathbf{X} \mathbf{\Gamma} \mathbf{X}' \quad (7)$$

## 2.2 Optimization problem

The network we have just introduced allows measuring systemic risk with several alternative approaches. At this stage, we consider our general objective function to be an aggregate measure of systemic risk, denoted as  $\Psi(\mathbf{X}, \mathbf{\Gamma}, \mathbf{B})$ , defined on the portfolio exposure matrix  $\mathbf{X}$ , the price impact matrix  $\mathbf{\Gamma}$ , and the spillover matrix  $\mathbf{B}$ . To preserve economic comparability between the optimal solutions and the status quo, we follow the approach proposed by Diem et al. (2020) and Pichler et al. (2021). Specifically, we restrict the search space to alternative configurations of the matrix  $\mathbf{X}$  that keep total assets for each bank and total outstanding amount for each asset

unchanged. This is ensured by imposing linear equality constraints on the row and column sums of the matrix. Additionally, we do not allow short positions by imposing non-negativity constraints. In mathematical terms, we can introduce a set of feasible systems  $\mathcal{F}(\mathbf{X})$  defined by the following constraints:

$$\mathcal{F}(\mathbf{X}) = \left\{ \mathbf{X} \in \mathbb{R}^{N \times K} : \sum_{k=1}^K x_{ik} = d_i, \quad \sum_{i=1}^N x_{ik} = s_k, \quad x_{ik} \geq 0 \quad \forall i, k \right\} \quad (8)$$

where  $d_i$  are status-quo total assets for bank  $i$  (i.e., “demand” for assets from  $i$ ),  $s_k$  is status-quo outstanding amount for asset  $k$  (i.e., “supply” of asset  $k$ ). Therefore, our optimization problem can be expressed as:

$$\begin{aligned} \min_{x_{ik}} \quad & \Psi(\mathbf{X}, \mathbf{\Gamma}, \mathbf{B}) \\ \text{s.t.} \quad & \mathcal{F}(\mathbf{X}) \end{aligned} \quad (9)$$

As presented in (9), the optimization focuses solely on systemic risk as the objective function. This implies ignoring all other aspects of the system and assuming the role of a central planner whose sole goal is to minimize systemic risk. However, as noted above, there is a potential trade-off between systemic and individual risk for each portfolio, primarily driven by diversification. Various strategies can be employed to address this trade-off between individual and systemic risk within an optimization framework. For instance, Pichler et al. (2021) introduce a set of portfolio-level quadratic inequality constraints to ensure that the resulting individual risk does not exceed a certain threshold for each bank. Another approach is to evaluate aggregate exposure to individual risk by deriving an individual risk counterpart to  $\Psi(\mathbf{X}, \mathbf{\Gamma}, \mathbf{B})$ . Assuming that all relevant information about individual portfolio risk is incorporated in the covariance matrix of asset returns  $\mathbf{\Sigma}$ , an aggregate measure of individual risk within the system can be expressed as  $\Upsilon(\mathbf{X}, \mathbf{\Sigma})$ . Building on this, we construct a multi-objective constrained optimization problem using linear scalarization, where the objective function is a  $\alpha$ -weighted sum of the two risk components:

$$\begin{aligned} \min_{x_{ik}} \quad & (1 - \alpha) \Psi(\mathbf{X}, \mathbf{\Gamma}, \mathbf{B}) + \alpha \Upsilon(\mathbf{X}, \mathbf{\Sigma}) \\ \text{s.t.} \quad & \mathcal{F}(\mathbf{X}) \end{aligned} \quad (10)$$

where  $\alpha \in [0, 1]$ , such that the objective function is a convex combination of systemic risk  $\Psi(\mathbf{X}, \mathbf{\Gamma}, \mathbf{B})$  and aggregate individual risk  $\Upsilon(\mathbf{X}, \mathbf{\Sigma})$ . The value of  $\alpha$  indicates the relative preference for minimizing systemic or individual risk in the system, where  $\alpha = 0$  corresponds to minimizing systemic risk and  $\alpha = 1$  to minimizing individual

risk. By varying  $\alpha$ , we are able to find a Pareto frontier between individual and systemic risk in the banking system, which can be used as a tool for multi-criteria decision making, to evaluate existing structures in terms of their distance from the preferred combinations of the two measures, and to study how optimal portfolio structures change between the two extremes. The way the optimization problem can be addressed differs depending on the choice of the objective function, which we introduce in the next section.

## 3 Data and methodology

### 3.1 Description of the data

We apply our optimization framework to the European Banking System, using the data on banks' sovereign exposures published under the annual EBA Transparency Exercise and generally reported on a semi-annual basis as end-of-semester exposures. From the original EBA dataset, we select a sample of 49 banks from 10 EMU countries and 27 country-specific sovereign assets. We supplement the data with information on traded volumes and government bond indices, collected from various sources. Our central assumption is that all assets in banks' portfolios are marked to market. This may be an overly simplistic assumption, as the EBA items for which a counterpart country breakdown is available include both securities and loans. For this reason, we refer to Duarte and Eisenbach (2021), who show that the evolution of systemic risk from overlapping portfolios is not significantly affected by the inclusion of loans in the fair value portfolio. Further details on the data sources and operations on the sample are provided in B. Overall, our analysis covers about 70 percent of the total sovereign exposures reported by EBA for the first semester of 2023 (2023-1).

The application to the European case is relevant because of the large absolute size of sovereign assets held by European banks (EUR 3.4 tn in June 2023), and because they represent a large share of total assets (on average, around 10%). Furthermore, European banks' significant investment in home country sovereign exposures poses challenges due to the so-called bank-sovereign doom loop, as sovereign stress can be amplified by banks' holdings of government debt (Altavilla et al., 2017). Figure 2 shows total sovereign exposures for the sample considered (left scale), together with their relative share of total assets (right scale) for 2023-1. We also report the heatmap of EBA status quo portfolios for the same period in Figure 3, which suggests that while most sovereign exposures are held in relatively small amounts in banks' portfolios, some assets play a dominant role, notably exposures to the largest EMU countries (FR, ES, IT and DE) and US securities. The issue of sovereign portfolio allocation and diversification is particularly relevant for European banks,

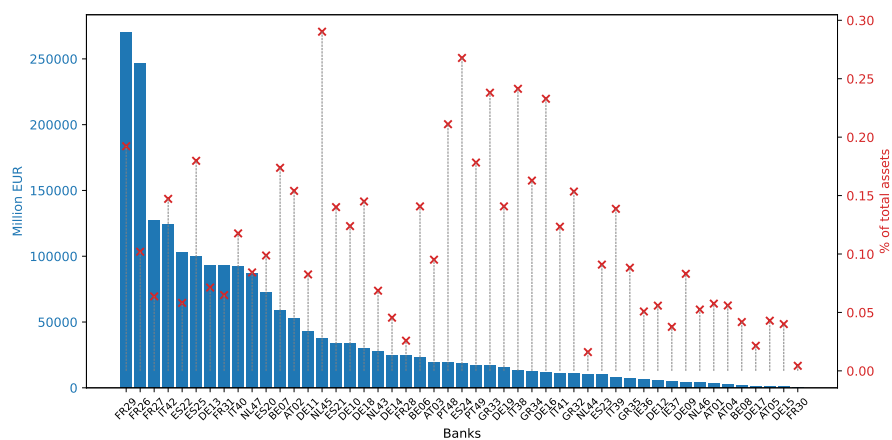


**Figure 2:** Sovereign exposures descriptives (2023-1). Total sovereign portfolio for each bank, ranked in descending order of size (left scale). The red crosses (right scale) represent total sovereign portfolios as a share of total assets.

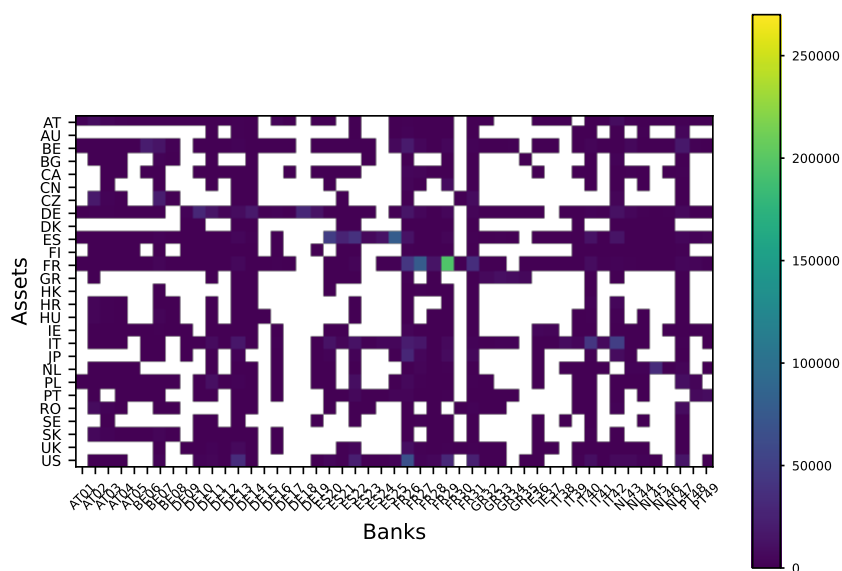


**Figure 3:** EBA sovereign portfolios (Million EUR, 2023-1). The columns of the heatmap represent banks' portfolios. Blank cells correspond to values exactly equal to 0.

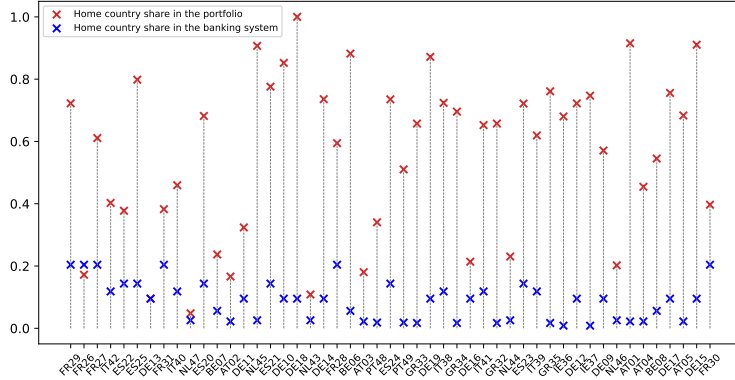


**Figure 4:** Home bias in sovereign exposures (2023-1). The red crosses represent the observed portfolio share of home country assets for each bank, while the blue crosses represent the corresponding shares in the banking system. The latter are the theoretical shares under perfect diversification and are calculated as the ratio of the total outstanding amount of home country assets to the total outstanding amount of sovereign assets held by all banks in the system.

as they invest a relatively large share in home country exposures, indicating the existence of a home bias in investment decisions. In Figure 4 we compare the observed home country investment shares with perfect diversification shares, i.e. the shares that banks would hold if they invested in assets in proportion to their outstanding shares in the system. The data shows that, for most of the banks in our sample, the observed home country shares are significantly higher than the theoretical counterpart. On average, the former is 14 times the latter as of June 2023.

### 3.2 Network estimation

To estimate price impacts  $\gamma_k$ , we follow a common liquidity-weighted portfolio overlaps model as developed by Cont and Schaanning (2019), and express the price impact parameter as<sup>5</sup>:

$$\gamma_k = \frac{1}{D_k} \quad (11)$$

where  $D_k$  is the market depth for security  $k$ , that we compute as:

$$D_k = c \frac{AV_k}{\hat{\sigma}_k} \sqrt{\tau} \quad (12)$$

<sup>5</sup>Other works use different specifications, such as the square root shape (Bouchaud, 2010) and exponential shape (Cifuentes et al., 2005). For a review, see Cont and Schaanning (2017). However, our optimization results are not significantly affected by different price impact assumptions, as shown in Figure A.3. Therefore, we maintain the linear specification for ease of explanation.

where we assume a liquidation period of  $\tau$  days,  $AV_k$  is the daily average trading volume,  $\hat{\sigma}_k$  is the realized volatility of daily returns, and  $c$  is set to 0.3 following Cont and Schaanning (2017) and Obizhaeva (2012). In summary, the market depth is such that selling a nominal amount  $D_k/100$  of asset  $k$  causes a 1% impact on its price.

Various methods can be used to evaluate spillovers. In this setting, our aim is to assess the impact of a price change in an asset affected by fire sales on other assets that are not directly impacted by such sales. To address the estimation, in order to account for the presence of systematic components potentially inducing correlation between assets, we adopt a node-wise regression approach using an elastic-net penalty (Zou and Hastie, 2005), as suggested in Meinshausen and Bühlmann (2006), and formulated in Yuan (2010) and Bernardini et al. (2022). More specifically, given the assumption of multivariate normality of asset returns, we model the distribution of the return on asset  $k$ , conditional on the vector  $\mathbf{r}_{-k}^t$  of the remaining  $K - 1$  asset returns, using the following linear relationship:

$$r_k^t | r_{-k}^t = \alpha_k + \mathbf{r}_{-k}^t \beta_k + \varepsilon_k \quad k = 1, \dots, K \quad (13)$$

The adopted approach consists of estimating regression (13) for each asset, thus obtaining  $K$  vectors  $\beta_k$  having  $(K - 1)$  elements  $\beta_{kl}$ . We then augment all vectors  $\beta_k$  by appending a 1 at position  $k$  and combine them row-wise to obtain  $\mathbf{B}$ , a  $K \times K$  matrix with ones along the diagonal. We estimate regressions (13) on the daily returns of government bond indices at semi-annual windows<sup>6</sup>, selecting the amount of penalty by means of 5-fold cross-validation. Since we do not have further information on the cross-section of government bond index returns, we adopt a balanced approach and set the parameter controlling the trade-off between LASSO and Ridge penalization to  $l1 = 0.5$ , corresponding to an equal weight assigned to each penalty.<sup>7</sup> While they are not the only alternative for estimating spillovers (Diebold and Yilmaz, 2008; Billio et al., 2012; Anufriev and Panchenko, 2015; Barigozzi and Brownlees, 2019), we choose node-level elastic-net regressions because they allow robust estimation of directed linkages (expressed by the coefficients  $\beta$ ) under highly correlated regressors (Zou and Hastie, 2005) and a sparse underlying dependence structure. In our application, we estimate return dependence in government bond markets under normal market conditions. Price spillovers, as modeled by Greenwood (2005), arise when temporary changes in asset prices due to non-fundamentally related sales are transmitted to temporary price changes in other assets unaffected by

---

<sup>6</sup>See Table B.1 for details on data sources.

<sup>7</sup>We have also checked the out-of-sample performance for different values of the  $l1$  ratio between 0 and 1. However, the tests do not show a clearly better performance for any specific value, thus leading us to adopt such a perfectly balanced approach.

the sales, due to arbitrageurs’ hedging operations. Because they occur in exceptional events, a more accurate estimate of such spillovers would require an event-study approach. However, event-study estimates would be difficult to extend for forecasting purposes. To the best of our knowledge, no study provides an estimate of such spillovers except Greenwood (2005), who tests his model on a redefinition event for the Nikkei 225 index. For this reason, we follow the approach described above and assume that the estimated matrix  $\mathbf{B}$  holds for fire sales as well. Our goal is simply to compare the level of systemic risk with and without spillovers under a given conditional distribution of asset returns and to find the corresponding optima.

### 3.3 Risk measures

Based on the network model introduced in Equation (7), in this section we present the measures adopted for both systemic and individual risk and outline the optimization strategy. Recent literature has introduced a number of different approaches to the definition and quantification of systemic risk in a portfolio overlap setting, encompassing both aggregate and individual bank or asset levels. Caccioli et al. (2014) employ what we refer to, for simplicity, as a “stability approach” to systemic risk. This approach focuses on assessing the probability and extent of contagion within a financial system through analytical evaluations of stability properties in indirect link networks. The method is based on the analysis of the principal eigenvalue of a matrix containing the probability of default in a branching process. They show that this approach performs well in predicting the probability and extent of contagion in a given system. Cont and Schaanning (2019) also adopt a stability approach to systemic risk, and introduce measures of bank-level systemicness based on eigenvector centrality computed on the weighted adjacency matrix. An alternative and widely used approach to measuring systemic risk is based on quantifying losses from indirect contagion under different assumptions about fire sales, deleveraging behavior, and initial shocks. Greenwood et al. (2015) introduce a measure of aggregate vulnerability (AV) as the sum of potential losses that the system would suffer as a result of a shock to asset returns relative to total capital. Similar measures are also presented in Braverman and Minca (2018) and Duarte and Eisenbach (2021). While aggregate vulnerability, as defined in Greenwood et al. (2015), accounts for first-round contagion losses due to bank deleveraging, Poledna et al. (2021) adapt Battiston et al. (2012)’s DebtRank to a network of indirect connections. This measure, through an iterative algorithm, quantifies the losses incurred by the system in subsequent rounds of contagion under a linear deleveraging scenario and asset sales proportional to portfolio weights. Similar approaches are also used in Cao et al. (2021) and Cont and Schaanning (2017).

In this paper, we define aggregate systemic risk as the total amount of portfolio overlap in the system, which provides a measure of the maximum potential losses that banks could suffer in the event of fire sales. This choice is motivated by Pichler et al. (2021), who use a first-round approximation of DebtRank, where exposures are scaled by equity, and find that optimized structures are also more resilient to subsequent rounds of losses. Thus, for the baseline case without cross-sectional spillovers, we define our systemic risk function as the sum of portfolio overlaps in the system:

$$\Psi^{aff} = \sum_i \sum_{j \neq i} w_{ij}^{aff} = \sum_i \sum_{j \neq i} \sum_k x_{ik} \frac{1}{D_k} x_{jk} \quad (14)$$

while the extended version, including the spillovers to unaffected assets, is computed as:

$$\Psi^{tot} = \sum_i \sum_{j \neq i} w_{ij}^{tot} = \sum_i \sum_{j \neq i} \sum_k \sum_l x_{ik} \frac{1}{D_k} \beta_{lk} x_{jl} \quad (15)$$

In both versions, we exclude fire-sales haircuts, i.e., losses banks would cause to the residual assets of their own portfolio, by selling a part of it. Equation (15) corresponds to the sum over all elements of the matrix:

$$\mathbf{W} - \text{diag}(\mathbf{W})$$

The measure proposed in (14) is in line with standard aggregate vulnerability measures. We can reformulate (15) as the sum of two components:

$$\Psi^{tot} = \underbrace{\sum_i \sum_{j \neq i} \sum_k x_{ik} \frac{1}{D_k} x_{jk}}_{\Psi^{aff}} + \underbrace{\sum_i \sum_{j \neq i} \sum_k \sum_{l \neq k} x_{ik} \frac{1}{D_k} \beta_{lk} x_{jl}}_{\Psi^{unaff}} \quad (16)$$

where the first term measures the total amount of portfolio overlap due to holdings of the same asset. Contagion in this component is due to the price impact of sales of the affected assets. The second term is a measure of the amount of portfolio overlaps due to the potential price impact of spillovers to unaffected assets. While the first component is always positive and, except for perfectly symmetric systems, has a minimum non-eliminable part, the contribution of the second component to the total portfolio overlaps will vary depending on the conditional distribution of asset returns. The linear specification of the price impact function can cause prices to fall below zero. For this reason, we cap the price impacts at 1 in the implementation of the objective function. Except for the case where a single bank's holding of asset  $k$  is larger than market depth, the overlapping portfolio network will be symmetric, as  $w_{ij} = w_{ji}$ .

As for the individual risk component  $\Upsilon$ , to ensure the possibility of measur-

ing individual risk in nominal terms, as is the case for (14) and (15), we adopt a Value-at-Risk approach under asset returns normality assumptions. Therefore, bank  $i$ 's individual risk can be measured as the period portfolio Value-at-Risk at the  $p$  confidence level:

$$VaR_i^p = -z_p \cdot \sigma_i \cdot d_i = -z_p \cdot \sqrt{\sum_{k=1}^K \sum_{l=1}^K \omega_{ik} \omega_{il} \sigma_{kl}} \cdot d_i \quad (17)$$

where  $\sigma_i$  is bank  $i$ 's portfolio standard deviation and  $d_i$  is its total portfolio value, introduced in (8), while  $\omega_{ik}$  and  $\omega_{il}$  are, respectively, the weights assigned to assets  $k$  and  $l$  in  $i$ 's portfolio, and  $\sigma_{kl}$  is the  $(k, l)$ -th element of the covariance matrix  $\Sigma$ . Besides allowing direct comparability with systemic risk measures<sup>8</sup>, the choice of Value-at-Risk as individual risk measure is motivated by existing theoretical models entailing VaR-based risk regulation (Acharya, 2009; Ibragimov et al., 2011; Adrian and Shin, 2013). Based on individual  $VaR$  measures, we define our aggregate measure of individual risk as the period aggregate Value-at-Risk in the system, computed as the sum of individual  $VaR$ s:

$$\Upsilon(\mathbf{X}, \Sigma) = \sum_{i=1}^N VaR_i^p \quad (18)$$

### 3.4 Optimization strategy

Previous work has proposed several alternatives to perform the systemic risk minimization. For direct network optimization, Diem et al. (2020) formulate the problem as a standard mixed-integer linear program, while in a similar application Krause et al. (2021) use a stochastic optimization algorithm. For portfolio overlap networks, Pichler et al. (2021) show that the optimization problem can be expressed as a quadratic program. All of these works take a systemic risk measure as the objective function of the problem, with constraints imposed on marginal quantities (i.e., row and column sums of the network matrix) and individual risk-return indifference constraints. The aim of our analysis is to investigate how portfolio allocation should be structured to minimize systemic risk and to evaluate the system's properties under different preferences for systemic and individual risk. As a result, the number of optimizations we need to perform is significantly larger than a one-time systemic risk optimization. In addition, our  $\alpha$ -weighted objective function introduced in (??) cannot be easily accommodated in standard formulations, and the non-convex na-

<sup>8</sup>Direct comparison of (18) with (14) and (15) requires caution in any case. In fact, while the former is an expected maximum loss the portfolio would experience, in the reference period, with a given degree of confidence, the latter represents the maximum amount of losses if banks liquidate all their assets at the same time.

ture of the systemic risk function complicates the adoption of standard optimization tools. For these reasons, we introduce an evolutionary search algorithm to solve the problem (10). The algorithm performs a non-deterministic heuristic optimization using an evolutionary search strategy that employs a mutation approach to explore the solution space. More specifically, at each iteration, a population of feasible solutions is generated by a constrained mutation process and evaluated according to the given objective function. The algorithm randomly initializes solutions and iteratively mutates them, updating the current solution when a better one is found. Threshold acceptance is used to adjust the acceptance criterion during evolution. In addition, different initialization methods are used to escape local optima. This method allows the use of different types and combinations of objective functions to obtain optimal networks under different degrees of preference over the components as in (10). This approach guarantees flexibility in the definition of the objective functions and the assumptions underlying the network model. In addition, the execution time is significantly reduced, allowing the comparison of different optimal structures.<sup>9</sup>

In the following analyses, we proceed as follows. After providing analytical insights into the shape of the objective function and optimization solutions for a small toy system, we apply our approach to the data by first optimizing the constrained objective function defined in (14) under the constraints set in (8). To compare optimal solutions with and without cross-sectional spillovers, we provide the optimized solution for the extended formula (15) under the same constraints to maintain comparability. Both solutions consider only potential losses due to contagion, as the diagonal elements of the matrix  $\mathbf{W}$  are set to zero, and ignore banks' own exposures to fire-sale haircuts. We compare the systemic risk-optimal allocations with the individual risk-optimal allocations obtained by minimizing (18). Finally, we solve problem (10) using both the standard and spillover-augmented systemic risk function by varying the coefficient  $\alpha$  between 0 and 1. The solutions to the  $\alpha$ -weighted problem allow us to characterize a Pareto frontier between systemic and individual aggregate risk, where solutions with  $\alpha = 0$  correspond to the systemic risk-optimal structures, while solutions with  $\alpha = 1$  coincide with the individual risk-optimal structures.

---

<sup>9</sup>For more details on the technical aspects of the implementation and the pseudocode of the algorithm, see D.

## 4 Optimal solutions for toy systems

Before presenting the results of the empirical application, we discuss the analytical aspects of the objective functions introduced earlier and their implications for portfolio optimization within a simplified toy model. More detailed derivations are given in C. We begin by considering a simplified financial system consisting of two banks and two assets. Banks 1 and 2 have total assets  $d_1$  and  $d_2$ , respectively, while the assets in the system have total outstanding amounts  $s_1$  and  $s_2$ . By including constraints on the total assets of the banks, we can represent the system using the portfolio matrix:

$$\mathbf{X} = \begin{bmatrix} x & d_1 - x \\ y & d_2 - y \end{bmatrix}$$

Using this representation, we solve the optimization problem for the limiting cases of pure systemic risk minimization ( $\alpha = 0$ ) and pure individual risk minimization ( $\alpha = 1$ ), assuming the absence of cross-sectional spillovers. The objective function  $\Psi^{aff}(x, y)$  is concave under the feasible set  $\mathcal{F}$ , leading to a corner solution for the systemic risk minimization problem. Figure 5 (Panel (a)) provides a graphical illustration of  $\Psi^{aff}$  for the case  $2 \times 2$ , with parameters set such that  $d_1 < s_1 < s_2 < d_2$  and  $\gamma_1 > \gamma_2$ . The solution to the minimization is at the point:

$$x_{\Psi}^* = x_{11, \Psi}^* = d_1 \quad \text{and} \quad y_{\Psi}^* = x_{21, \Psi}^* = s_1 - d_1$$

while the banks' exposures to asset 2 can be derived from the constraints as  $x_{12, \Psi}^* = 0$  and  $x_{22, \Psi}^* = d_2$ . At the systemic risk optimum, the least liquid asset 1 is concentrated as much as possible in the portfolio of bank 1, and only the remaining outstanding amount is allocated to bank 2, which is able to invest fully in the total outstanding amount of asset 2. Therefore, the only portfolio overlap generated at the optimum depends on the remaining outstanding amount of asset 1. Panel (b) of Figure 5 shows the plot for individual risk  $\Upsilon(x, y)$  as a function of  $x$  and  $y$ , assuming  $\sigma_1^2 > \sigma_2^2 > \sigma_{12}$ . We can show that the solution to the first-order conditions for the independent  $\Upsilon$  minimization under the feasible set  $\mathcal{F}$  is the maximum entropy (ME) allocation:

$$x_{\text{ME}}^* = \left( \frac{s_1}{s_1 + s_2} \right) d_1 \quad \text{and} \quad y_{\text{ME}}^* = \left( \frac{s_1}{s_1 + s_2} \right) d_2$$

which corresponds to distributing portfolio weights of each asset in proportion to its relative outstanding amount in the system. Under a wide range of problem parameters, individual risk is a strictly convex function of  $x$  and  $y$ , and the ME allocation is the unique solution to the minimization problem. In Panel (a) of Figure 5, we also plot the value of  $\Psi^{aff}$  for the ME allocation  $(x^{\text{ME}}, y^{\text{ME}})$ , showing

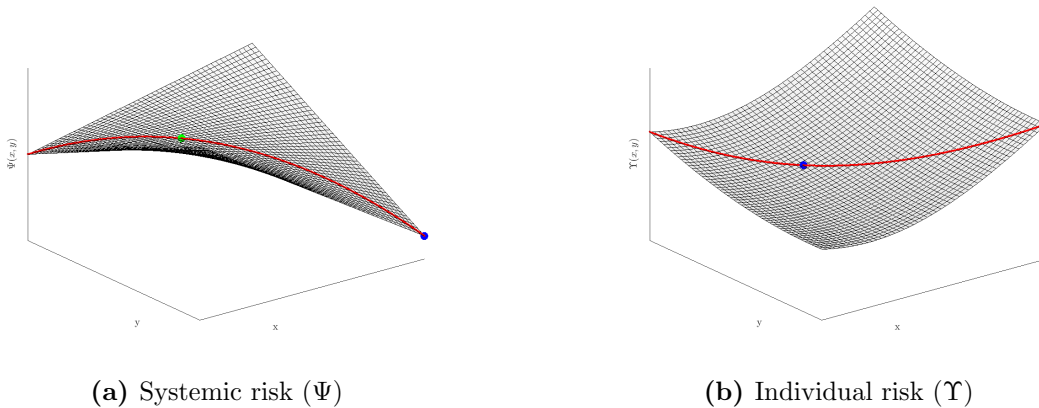


**Figure 5:** Surface and feasible set. Surface plots for the objective functions  $\Psi(x, y)$  (a) and  $\Upsilon(x, y)$  (b) over a restricted range of values for the dependent variables. The feasible set of values for  $x$  and  $y$  is represented by the red curve. The parameters are set such that  $d_1 < d_2$ ,  $s_1 < s_2$ ,  $\gamma_1 > \gamma_2$ , and  $\sigma_1^2 > \sigma_2^2 > \sigma_{12}$ . Minimum points are shown as blue dots, corresponding to a corner solution for systemic risk and the maximum entropy allocation for individual risk. The systemic risk associated with the maximum entropy allocation is also shown as a green dot in Panel (a), which is shown to be very close to the maximum for the objective function under the feasible set.

its proximity to the maximum systemic risk level under the feasible set.

Overall, the analysis of a small system provides useful insights into the shape of the objective functions and the direction of the solutions to the separate individual and systemic risk minimization problems. First, it shows that portfolios that minimize systemic risk are maximally concentrated. In the limiting case of a perfectly symmetric system, where  $d_1 = d_2$  and  $s_1 = s_2$ , optimal portfolios would be isolated with no overlap, while the degree of liquidity of the assets would not be relevant to the solution. If some overlap is necessary due to asymmetries in the system, then the comparative evaluation of asset size and liquidity will determine which assets are better isolated and which can be shared by different portfolios. Since the solution lies in one of the corners of the problem, a comparison must be made between the values of the objective function at each corner. Second, aggregate individual risk minimization leads to fully diversified allocations. Portfolios in the individual risk optimum are perfectly homogeneous, and all banks allocate their holdings according to the same weights. In contrast, portfolios in the systemic risk optimum are characterized by extreme diversity in asset allocation. Finally, even in a small system such as the one under analysis, there is a clear trade-off between individual and systemic risk. As we show in Figure 5, the optimal solution for minimizing individual risk is close to the maximum point for systemic risk, and vice versa. Optimizing for one dimension of risk tends to exacerbate the other, suggesting a significant inefficiency in finding optimal solutions to each problem independently. Seeking only individual risk min-

imization will produce highly inefficient portfolios from a systemic perspective, and the same is true for systemic risk minimization alone. Therefore, this trade-off must be taken into account when evaluating portfolio allocations, and intermediate solutions could allow both dimensions to be addressed. Since the analytical derivation of an optimal solution that considers both objective functions does not have the nice properties of the functions just analyzed, we provide a more detailed treatment of the multi-objective optimization problem applied to the European case in the next section.

## 5 Empirical Results

### 5.1 Portfolio and network features at the optima

Figures 6 and 7 show a first set of optimization results for the sample of banks considered in the analysis. We denote the matrix portfolios resulting from the optimization of (14), (15), and (18) as  $\mathbf{X}_{\Psi,aff}^*$ ,  $\mathbf{X}_{\Psi,tot}^*$ , and  $\mathbf{X}_{\Upsilon}^*$ , while the portfolios resulting from the full multi-objective optimization (10) are denoted by  $\mathbf{X}_{\alpha}^*$ . The adjacency matrices of the resulting networks are denoted by  $\mathbf{W}_{\Psi,aff}^*$ ,  $\mathbf{W}_{\Psi,tot}^*$ ,  $\mathbf{W}_{\Upsilon}^*$ , and  $\mathbf{W}_{\alpha}^*$ . In particular, Figure 6 shows the optimal solutions  $\mathbf{X}_{\Psi,aff}^*$ ,  $\mathbf{X}_{\Psi,tot}^*$ , and  $\mathbf{X}_{\Upsilon}^*$  based on 2023-1 data, providing a first comparison with the status quo portfolios shown in Figure 3, while Figure 7 shows the corresponding portfolio overlap networks. These solutions coincide with the opposite extremes of problem (10), with  $\alpha$  set to 0 for Panels (a) and (b) and  $\alpha = 1$  for Panel (c) in both Figures. Systemic-risk optima (Panels (a) and (b) of Figure 6) show a high degree of portfolio concentration. Panel (c) shows the optimal matrix  $\mathbf{X}_{\Upsilon}^*$  for the individual risk optimization, which converges to the perfectly diversified solution introduced in section 4. Portfolio concentration in the systemic risk optima results in sparser networks in both cases, as shown in the first two panels of Figure 7, while the network of portfolio overlaps is complete for the individual risk optimal portfolios, reported in Panel (c). Network plots in Figure 7 show that the number of economically relevant connections is significantly higher for  $\mathbf{X}_{\Upsilon}^*$ , while most of connections arising in the optimal systems  $\mathbf{X}_{\Psi,aff}^*$  and  $\mathbf{X}_{\Psi,tot}^*$  take very small values.

A first aspect emerging from Figure 6 is the significant difference in portfolio diversification. Systemic-risk optimal portfolios appear to be highly concentrated both for the standard model and for the one including spillovers, and network overall topological features are preserved in both versions. In fact, the inclusion of spillovers only affects the choice of which assets can be diversified more at the optimum (e.g., see differences for UK government bonds). Since the shape of the results does not change significantly between the two versions of the problem in the European case,

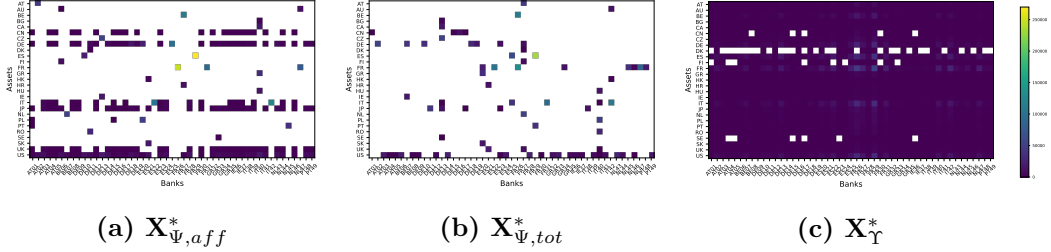


**Figure 6:** Optimized portfolios (Million EUR, 2023-1). (a) Optimal portfolio structures obtained by minimizing  $\Psi^{aff}$  ( $\alpha = 0$ ). (b) Optimal portfolio structures obtained by minimizing  $\Psi^{tot}$  ( $\alpha = 0$ ). (c) Optimal portfolio structures obtained by minimizing  $\Upsilon$  ( $\alpha = 1$ ). Empty cells correspond to values exactly equal to 0.

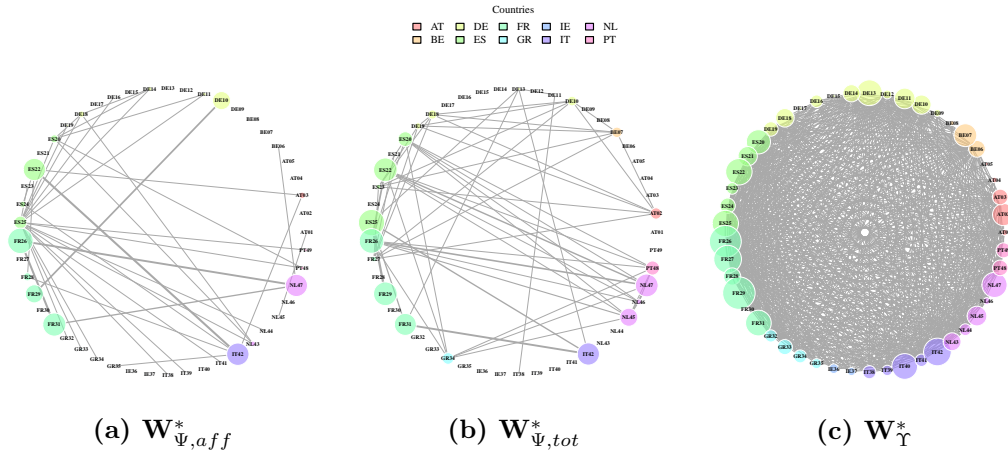


**Figure 7:** Optimized networks (2023-1). Weighted undirected plot of portfolio overlap networks resulting from optimal structures under (a)  $\Psi^{aff}$ , (b)  $\Psi^{tot}$ , and (c)  $\Upsilon$ . All links are estimated excluding cross-sectional spillovers between different assets and assuming daily liquidation ( $\tau = 1$ ). To improve readability, edges with values less than EUR 100,000 are not shown in the graphs.

we provide details and comments mainly for the standard model without spillovers. For the sample considered, the returns on sovereign assets show a mostly positive dependence structure, as shown in Figure A.1, where we report the estimated  $\mathbf{B}$  matrix for the last period available (2023-1). Therefore, price impacts generated by asset sales are transmitted to losses in prices of assets not affected by sales, thereby amplifying aggregate losses in the system. Under correlation patterns where a larger number of zero or negative components are present (e.g., including different asset classes), systemic risk amplification features would be less pronounced and would be partially offset by negative spillover components, as already pointed out in the description of (16). For this reason, possible extensions of this framework to simulated systems or to data with more asset classes would provide further insights into the behavior of different systems with respect to systemic risk. We believe these aspects deserve more attention, and we leave further analysis to future research.

In Table 1 we report summary statistics for the 2023-1 optimization results, comparing systemic and individual risk optimal structures (columns I to III) with the observed status quo data (column IV) and the maximum entropy (ME) system (column V). Part A of the Table reports the value of the objective functions normalized by total T1 capital of the system. The optimal allocations for systemic risk take the minimum values for the respective objective functions, while systemic risk is highest (almost identical) for the individual risk optimum and the ME matrix. Aggregate individual risk takes its smallest value for the respective optimum and the ME matrix, indicating almost complete convergence of the optimization algorithm to the maximum entropy portfolio allocation, and suggesting optimality of perfect diversification even for systems larger than  $2 \times 2$ . However, the values of  $\Upsilon$  for the other structures do not vary significantly. This fact suggests a large scope for systemic risk reduction without excessive deterioration of individual exposure to market risk for the case of European sovereign exposures. To provide a parallel to the  $2 \times 2$  case, we also ran maximization for both  $\Upsilon$  and  $\Psi^{aff}$  and found that the maximum value for  $\Upsilon^{99\%}$  with  $\tau = 20$  is about 8.1% of total capital, slightly higher than the corresponding value for the  $\Psi^{tot}$  optimum. The maximum value for  $\Psi^{aff}$  is 13.1% of total capital, which is also very close to the value registered under ME structures, confirming the suggestive evidence provided in the previous section.

Part B of Table 1 provides a comparison of portfolio statistics for the alternative structures considered. As a measure of portfolio diversification, we report the average Herfindahl-Hirschmann (HH) index for bank portfolios, computed as:

$$HH_i = \sum_k \left( \frac{x_{ik}}{d_i} \right)^2 \quad (19)$$

**Table 1:** Optimization results. Summary statistics for the optimization results (columns I-III), against the status quo (column IV) and the maximum entropy ( $\mathbf{X}_{ME}$ , column V) portfolios, obtained on the 2023-1 data. The objective function values in Part A are normalized by dividing by the sum of banks' T1 capital, for a liquidation period  $\tau = 20$ . Network statistics are computed for  $\tau = 1$ . The numbers in parentheses in part C are the average number of negative links per node.

	$\mathbf{X}_{\Psi,aff}^*$ (I)	$\mathbf{X}_{\Psi,tot}^*$ (II)	$\mathbf{X}_{\Upsilon}^*$ (III)	Status quo (IV)	$\mathbf{X}_{ME}$ (V)
<i>A. Objective functions values</i>					
$\Psi^{aff}$	0.030	0.043	0.127	0.109	0.128
$\Psi^{tot}$	0.202	0.173	0.288	0.272	0.288
$\Upsilon^{99\%}$	0.075	0.078	0.071	0.072	0.071
<i>B. Portfolio statistics</i>					
Average HH banks	0.45	0.89	0.11	0.44	0.11
Average HH assets	0.77	0.82	0.06	0.22	0.06
Average N. assets	4.24	1.57	26.04	14.34	27
Assets rebalancing required ( <i>l1</i> dist., %)	86.3	87.6	64.4	-	64.1
Average portfolio diversity	0.63	1.01	0.03	0.79	0
<i>C. Network statistics</i>					
Density	0.76	0.47	1	0.99	1
Average degree	36.4	22.6 (2.9)	48	47.7 (1.6)	48
Average DebtRank ( $\tau = 1, s = 1$ )	0.029	0.042	0.088	0.072	0.089

for each bank. The HH index takes values closer to 1 the more concentrated are the portfolios. Average diversification at the bank level is comparable between the optima and the status quo, and is highest (i.e., lowest HH index) for the individual risk optimum and the ME system. Therefore, from an average diversification perspective, status quo portfolios have allocations closer to systemic risk optima than individual risk ones. However, status quo portfolios contain a larger number of assets. We take a deeper look at portfolio diversification in Figure 8, reporting the distribution of banks' HH indexes for the different optimal structures  $\mathbf{X}_\alpha^*$  as the value of  $\alpha$  varies between 0 and 1, where  $\alpha = 0$  corresponds to the systemic-risk optimal structure while  $\alpha = 1$  to the individual risk optimal structure. The first observation reports the HH-distribution for the status-quo EBA system. European banks' sovereign portfolios show a high degree of variability in diversification, ranging from a HH index of about 0.12 to full concentration ( $HH = 1$ )<sup>10</sup>. Optimization also reduces variability in portfolio diversification levels. For systemic risk optimal structures ( $\alpha = 0$ ), while we observe comparable average HH indexes, the lower tail of the HH distribution is significantly shrunk, suggesting that highly diversified positions are inefficient from a systemic risk perspective. As we move towards individual risk optimal structures, diversification increases, until converging to a maximum entropy allocation where all banks hold the same shares of assets in their portfolios.

Overall, extreme diversification appears to be inefficient from a portfolio overlaps perspective, while the average diversification observed in the banking system is preserved under the optimization approach. Optimal portfolio diversification must be combined with targeted asset selection, as the connectivity structure is determined by the combination of asset allocation and asset liquidity. As also suggested by the analytical intuition, optimization tends to concentrate illiquid assets (i.e., those with the highest price impact coefficients) in the smallest possible number of portfolios, and to spread the “safest” assets, whose high degree of liquidity minimizes potential losses from exogenously driven fire sales. Certain structures of the system, in particular for banks' and assets' size distributions closer to uniform, however, still show maximum portfolio concentration at the optima.

The HH index may mask important structural differences in the composition of sovereign portfolios when comparing systemic risk optima and the status quo. This is mainly due to the influence of a significant home bias in banks' observed portfolio allocation. The large weight of home country exposures has the potential to skew

---

<sup>10</sup>Further analysis (not reported here) shows that banks of different size also have different degrees of portfolio concentration. On average, banks in the highest quartile of the portfolio size distribution show higher diversification (average HH around 0.3), while banks in the lower quartile have more than 1.5 times average concentration (average HH around 0.51).

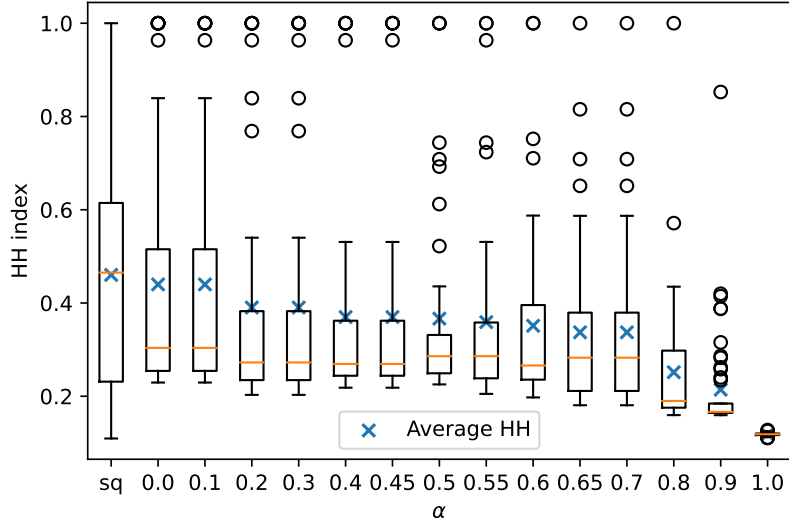


**Figure 8:** Portfolio HH index distribution. The first boxplot shows the HH index distribution for the status quo (sq) bank portfolios for 2023-1, while the following show optimal structures for values of  $\alpha$  ranging from 0 ( $\mathbf{X}_{\Psi,aff}^*$ ) to 1 ( $\mathbf{X}_{\Upsilon}^*$ ). Solutions are shown for the objective function based on  $\Psi^{aff}$ .

the HH index towards higher values. Consequently, this bias offsets the higher diversification observed in other assets in the status quo. To address this limitation, we further investigate portfolio diversification by analysing the Concentration Ratio ( $CR$ ) for the different portfolio allocations. The  $CR$  is computed as the cumulative sum of portfolio shares invested in the  $n$  largest assets within the portfolio. This provides a more accurate perspective on the distribution of portfolio shares and better captures the actual diversification profile. In our case, the concentration ratio for the largest  $n$  assets in the bank  $i$ 's portfolio is obtained as:

$$CR_n^i = \sum_{k=1}^n \frac{x_{ik}}{d_i}$$

for  $n = 1, \dots, K$ . Figure 9 shows that on average, although the largest asset receives a comparable share in the status quo, in systemic risk-optimal portfolios significantly higher shares are assigned to the next largest assets. This suggests a more concentrated portfolio on a few assets in the optimal structures compared to the status quo. As shown in part B of Table 1, on average, banks' systemic risk optimal portfolios (columns I and II) have around 4 assets, while in the status quo banks hold around 14 assets in the portfolios.

In Table 1, we also report the average asset-level HH index, which provides a measure of how much government assets are spread across banks' portfolios. On

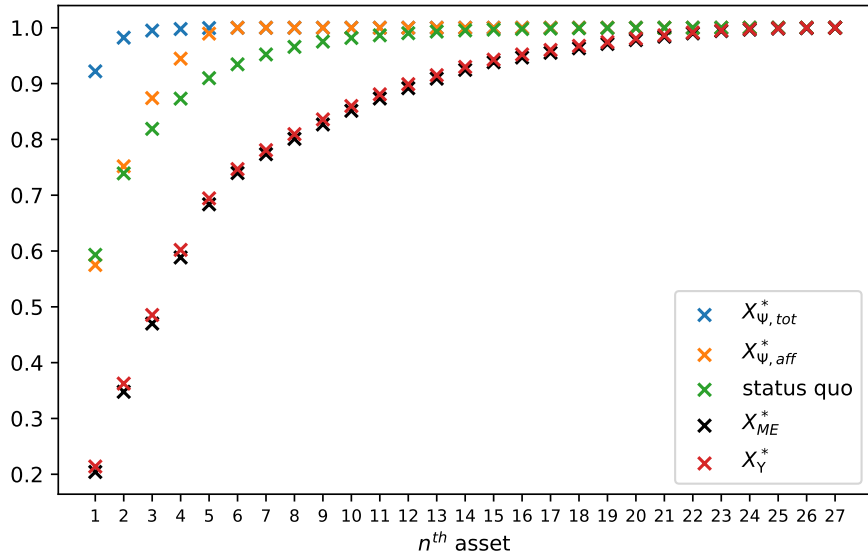


**Figure 9:** Average CR for bank portfolios. The crosses show the average  $CR_n$  for the different structures for all  $n$ . Assets are shown in decreasing order of size, so that for each  $n$ , the average cumulative share of the largest  $n$  assets is shown.

average, assets are much more spread across portfolios in the status quo than in the systemic risk optima, while concentration is lowest in the individual risk optimum. The concentration at the asset level is consistent with the tendency highlighted in the  $2 \times 2$  case: the choice of diversification depends on the size and liquidity of the assets, as suggested by Figure 6, where the most diversified assets in the system are the largest and most liquid. This is confirmed by Figure A.2, where assets are ranked by their relative market absorption capacity. While there is a general tendency toward concentration for all assets, the most liquid assets are still more diversified in the optimal system.

Differences in diversification and asset selection are reflected in the structure of the portfolio overlap networks. The first two rows of Section C of Table 1 show network density and average node degree for all structures considered. We compute node degree as the number of “active” edges (i.e., having a non-zero value) for each bank, as follows:

$$deg_i = \sum_{i \neq j} \mathbb{1}\{w_{ij} > 0\} \quad (20)$$

where  $\mathbb{1}\{\cdot\}$  is an indicator function that takes the value 1 when condition  $\cdot$  is met. Density is calculated as the ratio between the number of active edges and the maximum number of edges for the undirected version of the network. The ME and  $\Upsilon$  optimal portfolios generate a complete network of portfolio overlaps, while the  $\Psi^{aff}$  and  $\Psi^{tot}$  optimizations generate much sparser networks. Since some assets in the

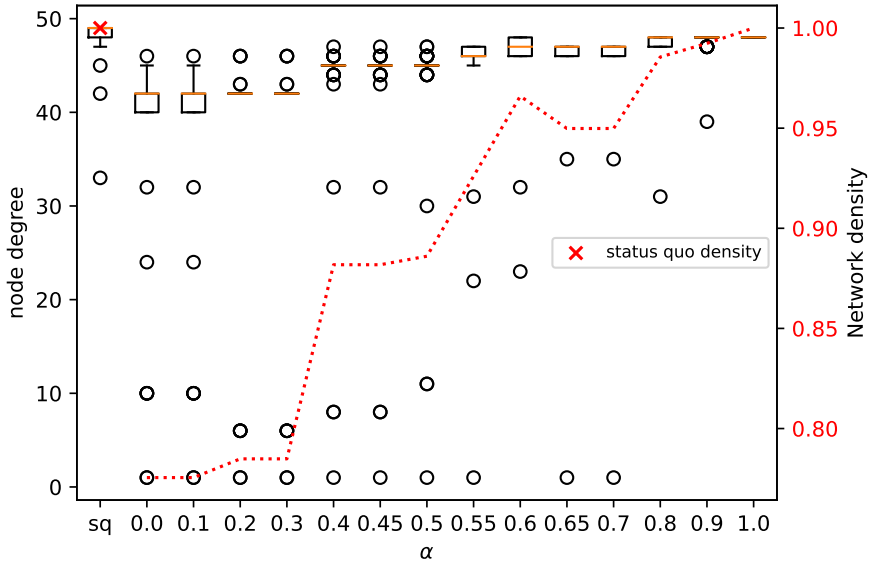


**Figure 10:** Node degree and network density for observed and optimal structures by varying  $\alpha$  (2023-1). The boxplots (right scale) show the degree distribution for the status quo portfolio overlap network (sq) and for  $\Psi^{aff}$ - $\Upsilon$  optimal structures for values of  $\alpha$  ranging from 0 ( $\mathbf{W}_{\Psi,aff}^*$ ) to 1 ( $\mathbf{W}_{\Upsilon}^*$ ). The red dotted line (right scale) represents the density for each network, computed as the ratio of the number of active connections ( $\sum_i deg_i$ ) to the total number of possible connections in the network (excluding self-exposures, the total number of possible connections is  $N \times N - N$ ).

market have negative correlations, the network derived using the full formula (7) has some negative links, highlighting the potential systemic risk-reducing role of negative asset correlations. The sparser network among those considered is produced by the  $\Psi^{tot}$  optimization, due to the higher contagion potential of positive correlations, which tends to move the optimal configurations toward higher concentration. In Figure 10 we show the degree distribution for the optimized networks by different levels of  $\alpha$  and for the status quo. The degree distribution for the observed data is significantly concentrated around full degree (where the maximum number of links for the EBA network is 48), while systemic risk optima have lower node degrees. As  $\alpha$  increases, diversification causes network density to increase, eventually leading to complete networks for  $\alpha$  close to 1. Overall, while portfolio diversification shows comparable values between the status quo and systemic risk efficient structures, concentration ratios and network densities reveals substantial differences. In the systemic risk-optimal structure, banks invest in fewer assets and network density is reduced by about 20%. Moreover, the status quo level of systemic risk is much higher than the optimal level. Thus, banks do not seem to take systemic risk into account in their portfolio allocation.

We finally look at how optimal networks perform under different rounds of con-

tagion. In part C of Table 1 we report DebtRank (Battiston et al., 2012) for each network, using the adaptation to portfolio overlaps settings proposed in Poledna et al. (2021). This measure is obtained as a result of an iterative process where each bank at a time is subject to a shock  $s$  to its equity (in our case we model bank failure, so we impose a shock  $s = 1$ ) and sells assets proportionally, in a linear deleveraging process. The contagion process runs until no more “distress” events occur.<sup>11</sup> The final value is the share of total assets in the system that is lost due to contagion. In our application, we simulated the failure of each bank separately and averaged across all banks. Although the average covers a wide range of values, the interesting aspect of this application is the fact that under optimized systems, the average losses in the case of contagion are about half of the losses incurred by the status quo system, confirming the good performance of optimizing first-round losses observed in Pichler et al. (2021) even under multiple rounds of contagion.

## 5.2 Distance measures

A crucial aspect of our problem is how close the observed portfolio allocations are to the optima. In the last row of part B of Table 1, we report the average amount of portfolio rebalancing needed to reach the corresponding structure from the status quo, calculated as half the  $l_1$  distance between the portfolio vectors in the considered structure and the portfolio vectors in the status quo. We multiply by 0.5 to avoid double counting, since due to the constraints on banks’ total assets, the amount of reduced positions must be exactly equal to the increase in other positions. Overall, the status quo portfolios are on average closer to the individual optimum than to the systemic risk optimum. The picture provided by the distance metrics also points to the significant portfolio rebalancing required to achieve optimal configurations. At the system level, Figure 11 shows the Frobenius distance between the status quo and the optima for different values of  $\alpha$ . Even assigning small weights to systemic risk in the weighted objective function can cause significant deviations from the status quo, suggesting potentially significant inefficiencies in the observed portfolio allocations. Systemic risk optimization, while minimizing the amount of portfolio overlap between banks, also increases portfolio diversity. In the last row of Part B, we report the degree of portfolio diversity for each system, computed as the average pairwise Euclidean distance between portfolios. The values of portfolio diversity are highest for the status quo and the systemic risk optima, while tending to zero for the individual risk optimum and for the maximum entropy portfolios.

---

<sup>11</sup>See Poledna et al. (2021) for a detailed description of the process.

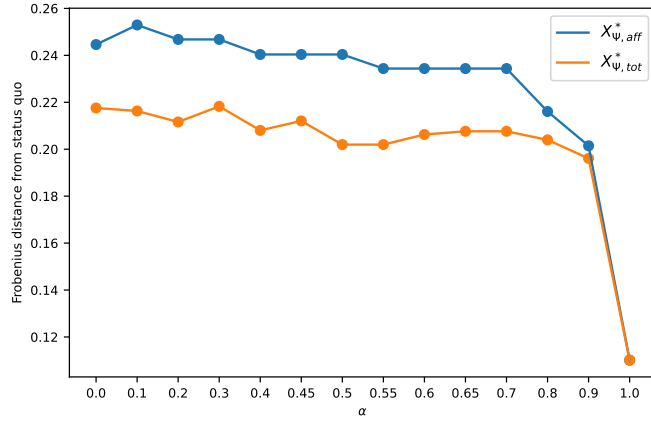


**Figure 11:** Frobenius distance from the status quo. The distance is computed as the Frobenius norm of the matrix difference between the status quo and the optima under the two objective functions  $\Psi^{aff}$  and  $\Psi^{tot}$ , scaled by the value of total assets. As we move from minimizing only systemic risk ( $\alpha = 0$ ) to minimizing individual risk ( $\alpha = 1$ ), the distance of the optimal structures from the status quo system decreases to almost half for  $\alpha = 1$  compared to the distance observed for  $\alpha = 0$ . This suggests a higher preference for individual risk reduction than for portfolio overlap control.

### 5.3 Pareto Frontiers

Figure 12 provides a summary of the optimization results for a selection of periods ranging from 2018-1 to 2023-1, for which we have already provided a more detailed analysis.<sup>12</sup> Results are represented as efficient individual-systemic risk frontiers, and a comparison is provided with the status quo values. For each frontier, the top-left point corresponds to  $\Upsilon$ -optima ( $\alpha = 1$ ), while the bottom-right point corresponds to  $\alpha = 0$  solutions. Two observations can be drawn by comparing the solutions to  $\Psi^{tot}$ - and  $\Psi^{aff}$ -minimization. On one hand, ignoring spillovers to unaffected assets does not significantly change the shape of the solutions. On the other hand, it would lead to a systematic underestimation of systemic risk in the presence of positive correlations. This difference is more pronounced in periods of high market volatility when positive correlations are stronger, as is the case for 2022-2. Comparing optimal values with status quo ones, we confirm that significant reductions in systemic risk are possible with limited deterioration in individual aggregate risk. This is the case, for example, for values of  $\alpha$  between 0 and 0.1. The status quo system shows a large room for improvement for all periods considered. In Figure 12, a “vertical” move towards the frontiers in the plot would dramatically reduce systemic risk, potentially without any deterioration in aggregate individual riskiness. A simple

<sup>12</sup>We considered these periods as case studies showing different market conditions. 2018-2 is the one with the lowest observed volatility in the market, while in 2020-1 and 2022-2 the highest volatilities have been recorded due to the COVID outbreak and global inflationary pressures, respectively. 2023-1 was chosen as the last available period.

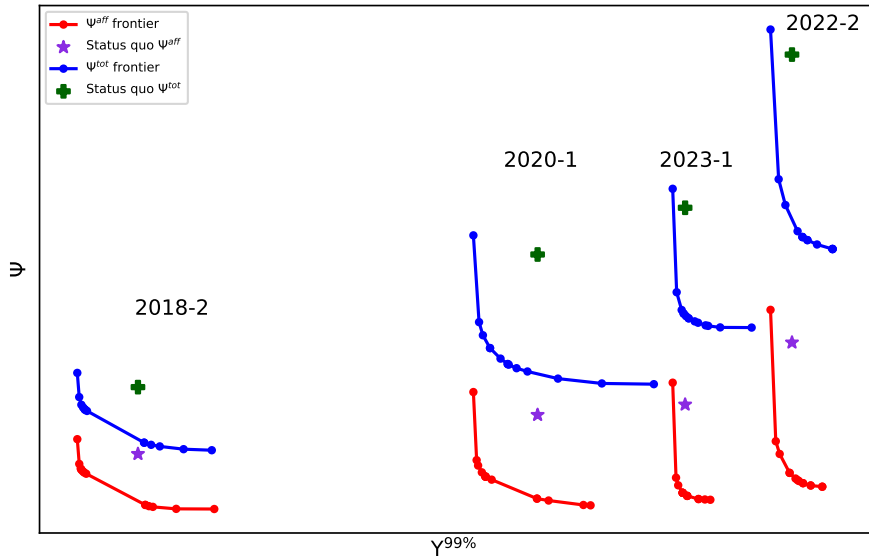


**Figure 12:** Evolution of  $\Psi$ - $\Upsilon$  efficient frontiers. The frontiers represent the combinations of  $\Psi^{aff}$ - $\Upsilon$  and  $\Psi^{tot}$ - $\Upsilon$  corresponding to optimal solutions under  $\alpha$  ranging from 0 (pure  $\Upsilon$  optima, upper-left point of the curves) to 1 (pure  $\Psi$  optima, lower-right point of the curves) for each selected period. The values of  $\Psi^{aff}$  and  $\Psi^{tot}$  are also displayed for the status quo portfolios for comparison.

numerical example can show the possibilities of improvement. Among the points in the  $\Psi^{aff} - \Upsilon$  frontier, the one having the closer value of  $\Upsilon$  to the observed data corresponds to  $\mathbf{X}_{0.5}^*$ , with  $\Upsilon^{99\%} = 7.2\%$  of total capital. Moving from the status quo to this intermediate optimum would entail rebalancing around 79 percent of the portfolio with no deterioration in individual risk, and a level of systemic risk equal to 3.4% of total capital, with a systemic risk reduction of around 69 percent compared to the status quo. The corresponding HH index, at the intermediate optimum, would be equal to 30.3%, thus producing more diversified portfolios with an average of 7.2 assets per bank.

## 6 Discussion of results

Taken together, the analyses presented so far reveal a number of important points. First, we show a clear trade-off between minimizing systemic risk, which would lead to highly concentrated portfolio allocations, and minimizing individual risk, which would result in maximally diversified portfolios. We address this trade-off by introducing a multi-objective evolutionary search framework, which allows us to characterize a set of efficient systemic-individual risk frontiers. Second, from an asset allocation perspective, our results show that diversification plays a crucial role in determining the level of systemic and individual risk. However, similar

aggregate levels of diversification may mask relevant differences in systemic risk, the actual level of which is jointly determined by asset size and liquidity. Nevertheless, in general, high levels of portfolio diversification are never observed in the optima, regardless of whether cross-sectional spillovers are ignored or included in the quantification of systemic risk. Ignoring spillovers may lead to a potential underestimation of systemic risk, even though it does not change the overall results. When there is a positive dependence among the asset classes in the portfolio, contagion might be amplified. Third, from a system assessment perspective, we show that the observed portfolio allocations are far from optimal and massive portfolio rebalancing would be required to reach the efficient frontier. However, the distance to minimum systemic risk is significantly larger than the distance to minimum individual risk. The large variation in systemic risk associated with the different optimal structures, compared to the smaller range of achievable individual risk levels, highlights the potential for a significant reduction in systemic risk without a deterioration in individual riskiness, for which we provide a numerical example. Finally, the problem we address poses significant analytical challenges. Although we can provide analytical intuition for small simplified systems, the non-convexity of systemic risk and the multi-objective framework require an adjusted numerical approach. The algorithm we present effectively addresses the issues raised by the structure of the problem due to its flexibility in formulation, limited computational time, and superior convergence properties compared to alternative solvers.

This paper is related to several previous works. Most directly, from a methodological perspective, it is related to recent contributions introducing network optimization approaches. In particular, our framework is applied to the same European sovereign exposure setting as Pichler et al. (2021), and we also find large scope for systemic risk reduction without individual risk deterioration. Compared to their approach, in addition to providing analytical intuition on the trade-off between the individual and systemic dimensions, we extensively analyze portfolio allocations for a wider range of combinations of systemic and individual risk. By employing a flexible heuristic optimization algorithm, our framework can be applied to a wider range of price impacts and objective functions, including multi-objective settings with non-standard formulations. We also extend standard portfolio overlap models to include the possibility of cross-sectional spillovers and find a potential underestimation of systemic risk for standard models. Regarding the role of diversification as a determinant of systemic risk, our results are also related to earlier work by Wagner (2010) and Ibragimov et al. (2011). However, while in these papers systemic risk is generated by exposures to common factors, in our setting systemic risk is the result of portfolio overlaps generated by diversification. In this respect, our general setup is consistent with Caccioli et al. (2014), who also suggest a potential negative effect

of diversification on financial stability, from a positive perspective. By focusing on optimal portfolio allocations from a central planner’s perspective and applying our framework to real data, we provide an empirical application related to recent theoretical results on optimal systemic diversification. Capponi and Weber (2024) find that maximum diversification at the individual level is inefficient when institutions incorporate the possibility of fire-sale losses in their portfolio optimization problem. On the one hand, our results also point to the systemic risk inefficiency of extreme diversification, which is never observed at the optimum. On the other hand, comparing the optima with the observed data, the status quo portfolios are far from being optimal in terms of systemic risk, even though average diversification is close to the optimal level. Banks invest in sovereign debt for a variety of reasons.<sup>13</sup> Nevertheless, their overall allocation appears to be driven more by individual Value-at-Risk than by systemic risk considerations. Moreover, the analysis of different time periods seems to suggest that banks do not adjust their portfolios towards VaR optimality at the same pace as market conditions, since the distance from the optimum tends to change as market conditions change.

## 7 Conclusion

The idea that diversification may have social costs in addition to individual benefits is not new to economic research. Recently, there has been an increasing interest in understanding how portfolio allocations behave with respect to systemic risk and which allocations are best for preserving financial stability. In this paper, we take this understanding a step further by investigating optimal allocations that take into account the two potentially conflicting dimensions of individual and systemic risk. The application to real-world data provides an empirical complement to recent theoretical studies and also offers some policy insights. First, it provides a rationale for policies aimed at improving market liquidity, which could help to contain the magnitude of losses resulting from market stress. Second, the highlighted trade-off between systemic and individual risk suggests that focusing on one dimension at a time may have unintended harmful effects on the other. Thus, rather than promoting unfocused diversification, incentives in asset selection — such as systemic risk taxes as in Acharya et al. (2013) or Poledna and Thurner (2016) — might work better to steer the system towards more stable configurations. Because of the substantial portfolio rebalancing required to achieve optimal configurations, optimization cannot be a policy solution for mitigating systemic risk. Still, it can provide useful information for evaluating observed allocations. We do so for the case of European sovereign

---

<sup>13</sup>See Dell’Ariccia et al. (2018) for an overview and further references.

exposures, which, though relevant, must be taken as a case study. Nevertheless, the flexibility of our framework lends itself to extensions that include more general cases with multiple asset classes, both on real and simulated data. Finally, further research is needed on the inclusion of cross-sectional spillovers, both on the mechanisms underlying the transmission of price impact and on the estimation of spillover matrices. The latter would benefit from more granular data at the security level, which could not be used for this application due to limitations in the granularity of portfolio holdings data.

## References

- Acemoglu, D., Ozdaglar, A., and Tahbaz-Salehi, A. (2015). Systemic risk and stability in financial networks. *American Economic Review*, 105(2):564–608.
- Acharya, V. V. (2009). A theory of systemic risk and design of prudential bank regulation. *Journal of Financial Stability*, 5(3):224–255.
- Acharya, V. V., Pedersen, L., Philippon, T., and Richardson, M. (2013). Taxing systemic risk. In *Managing and Measuring Risk*, pages 99–122. World Scientific.
- Adrian, T. and Shin, H. S. (2013). Procyclical leverage and value-at-risk. *Review of Financial Studies*, 27(2):373–403.
- Allen, F. and Gale, D. (2000). Financial contagion. *Journal of Political Economy*, 108(1):1–33.
- Altavilla, C., Pagano, M., and Simonelli, S. (2017). Bank exposures and sovereign stress transmission. *Review of Finance*, 21(6):2103–2139.
- Anufriev, M. and Panchenko, V. (2015). Connecting the dots: Econometric methods for uncovering networks with an application to the Australian financial institutions. *Journal of Banking & Finance*, 61:S241–S255.
- Awiszus, K., Capponi, A., and Weber, S. (2022). Market efficient portfolios in a systemic economy. *Operations Research*, 70(2):715–728.
- Barigozzi, M. and Brownlees, C. (2019). NETS: Network estimation for time series. *Journal of Applied Econometrics*, 34(3):347–364.
- Barucca, P., Mahmood, T., and Silvestri, L. (2021). Common asset holdings and systemic vulnerability across multiple types of financial institution. *Journal of Financial Stability*, 52:100810.
- Battiston, S., Puliga, M., Kaushik, R., Tasca, P., and Caldarelli, G. (2012). Debrank: Too central to fail? financial networks, the fed and systemic risk. *Scientific Reports*, 2(1).
- Beale, N., Rand, D. G., Battey, H., Croxson, K., May, R. M., and Nowak, M. A. (2011). Individual versus systemic risk and the Regulator’s Dilemma. *Proceedings of the National Academy of Sciences*, 108(31):12647–12652.
- Benoit, S., Colliard, J.-E., Hurlin, C., and Pérignon, C. (2017). Where the Risks Lie: A Survey on Systemic Risk. *Review of Finance*, 21(1):109–152.

- Bernardini, D., Paterlini, S., and Taufer, E. (2022). New estimation approaches for graphical models with elastic net penalty. *Econometrics and Statistics*.
- Billio, M., Getmansky, M., Lo, A. W., and Pelizzon, L. (2012). Econometric measures of connectedness and systemic risk in the finance and insurance sectors. *Journal of Financial Economics*, 104(3):535–559.
- Bouchaud, J. P. (2010). Price impact. *Encyclopedia of Quantitative Finance*.
- Braverman, A. and Minca, A. (2018). Networks of common asset holdings: aggregation and measures of vulnerability. *The Journal of Network Theory in Finance*, 4(3):53–78.
- Caccioli, F., Farmer, J. D., Foti, N., and Rockmore, D. (2015). Overlapping portfolios, contagion, and financial stability. *Journal of Economic Dynamics and Control*, 51:50–63.
- Caccioli, F., Shrestha, M., Moore, C., and Farmer, J. D. (2014). Stability analysis of financial contagion due to overlapping portfolios. *Journal of Banking & Finance*, 46:233–245.
- Cao, J., Wen, F., and Stanley, H. E. (2021). Measuring the systemic risk in indirect financial networks. *The European Journal of Finance*, 28(11):1053–1098.
- Capponi, A. and Weber, M. (2024). Systemic portfolio diversification. *Operations Research*, 72(1):110–131.
- Chernenko, S. and Sunderam, A. (2020). Do fire sales create externalities? *Journal of Financial Economics*, 135(3):602–628.
- Cifuentes, R., Ferrucci, G., and Shin, H. S. (2005). Liquidity risk and contagion. *Journal of the European Economic Association*, 3(2–3):556–566.
- Cont, R. and Schaanning, E. (2019). Monitoring indirect contagion. *Journal of Banking & Finance*, 104:85–102.
- Cont, R. and Schaanning, E. F. (2017). Fire sales, indirect contagion and systemic stress-testing. *Norges Bank Working Papers*, (2/2017).
- Dell’Ariccia, G., Ferreira, C., Jenkinson, N., Laeven, L., Martin, A., Minoiu, C., and Popov, A. (2018). Managing the sovereign-bank nexus. Departmental Paper 18/16, International Monetary Fund.

- Diebold, F. X. and Yilmaz, K. (2008). Measuring financial asset return and volatility spillovers, with application to global equity markets. *The Economic Journal*, 119(534):158–171.
- Diem, C., Pichler, A., and Thurner, S. (2020). What is the minimal systemic risk in financial exposure networks? *Journal of Economic Dynamics and Control*, 116:103900.
- Duarte, F. and Eisenbach, T. M. (2021). Fire-sale spillovers and systemic risk. *The Journal of Finance*, 76(3):1251–1294.
- Elliott, M., Golub, B., and Jackson, M. O. (2014). Financial networks and contagion. *American Economic Review*, 104(10):3115–3153.
- Ellul, A., Jotikasthira, C., and Lundblad, C. T. (2011). Regulatory pressure and fire sales in the corporate bond market. *Journal of Financial Economics*, 101(3):596–620.
- Falato, A., Hortaçsu, A., Li, D., and Shin, C. (2021). Fire-sale spillovers in debt markets. *The Journal of Finance*, 76(6):3055–3102.
- Freixas, X., Parigi, B. M., and Rochet, J.-C. (2000). Systemic risk, interbank relations, and liquidity provision by the central bank. *Journal of Money, Credit and Banking*, 32(3):611.
- Gai, P. and Kapadia, S. (2010). Contagion in financial networks. *Proceedings of the Royal Society A: Mathematical, Physical and Engineering Sciences*, 466(2120):2401–2423.
- Gilli, M., Maringer, D., and Schumann, E. (2019). *Numerical methods and optimization in finance*. Academic Press.
- Giudici, P., Sarlin, P., and Spelta, A. (2020). The interconnected nature of financial systems: Direct and common exposures. *Journal of Banking & Finance*, 112:105149.
- Glasserman, P. and Young, H. P. (2015). How likely is contagion in financial networks? *Journal of Banking & Finance*, 50:383–399.
- Greenwood, R. (2005). Short- and long-term demand curves for stocks: theory and evidence on the dynamics of arbitrage. *Journal of Financial Economics*, 75(3):607–649.

- Greenwood, R., Landier, A., and Thesmar, D. (2015). Vulnerable banks. *Journal of Financial Economics*, 115(3):471–485.
- Ibragimov, R., Jaffee, D., and Walden, J. (2011). Diversification disasters. *Journal of Financial Economics*, 99(2):333–348.
- Jackson, M. O. (2008). *Social and economic networks*. Princeton University Press.
- Jackson, M. O. and Pernoud, A. (2021). Systemic risk in financial networks: A survey. *Annual Review of Economics*, 13(1):171–202.
- Krause, S. M., Štefančić, H., Caldarelli, G., and Zlatić, V. (2021). Controlling systemic risk: Network structures that minimize it and node properties to calculate it. *Physical Review E*, 103(4).
- Meinshausen, N. and Bühlmann, P. (2006). High-dimensional graphs and variable selection with the lasso. *The Annals of Statistics*, 34(3).
- Newman, M. (2018). *Networks*. Oxford University Press.
- Obizhaeva, A. A. (2012). Liquidity estimates and selection bias. *Available at SSRN*.
- Pichler, A., Poledna, S., and Thurner, S. (2021). Systemic risk-efficient asset allocations: Minimization of systemic risk as a network optimization problem. *Journal of Financial Stability*, 52:100809.
- Poledna, S., Martínez-Jaramillo, S., Caccioli, F., and Thurner, S. (2021). Quantification of systemic risk from overlapping portfolios in the financial system. *Journal of Financial Stability*, 52:100808.
- Poledna, S., Molina-Borboa, J. L., Martínez-Jaramillo, S., van der Leij, M., and Thurner, S. (2015). The multi-layer network nature of systemic risk and its implications for the costs of financial crises. *Journal of Financial Stability*, 20:70–81.
- Poledna, S. and Thurner, S. (2016). Elimination of systemic risk in financial networks by means of a systemic risk transaction tax. *Quantitative Finance*, 16(10):1599–1613.
- Shleifer, A. and Vishny, R. (2011). Fire sales in finance and macroeconomics. *Journal of Economic Perspectives*, 25(1):29–48.
- Wagner, W. (2010). Diversification at financial institutions and systemic crises. *Journal of Financial Intermediation*, 19(3):373–386.

- Yellen, J. L. (2013). Interconnectedness and Systemic Risk : Lessons From the Financial Crisis and Policy Implications : Remarks at the American Economic Association/American Finance Association Joint Luncheon, San Diego, California.
- Yuan, M. (2010). High dimensional inverse covariance matrix estimation via linear programming. *Journal of Machine Learning Research*, 11(79):2261–2286.
- Zou, H. and Hastie, T. (2005). Regularization and variable selection via the elastic net. *Journal of the Royal Statistical Society Series B: Statistical Methodology*, 67(2):301–320.

## A Additional Figures

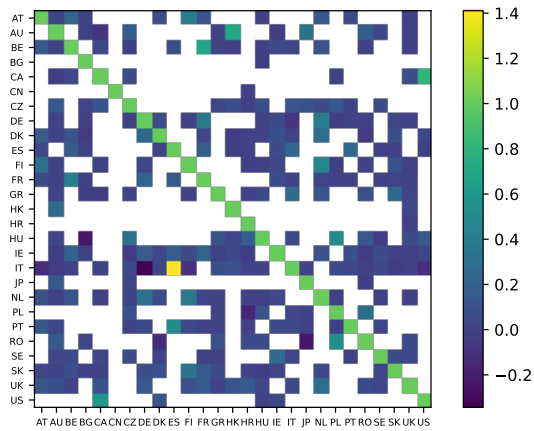


**Figure A.1:** Estimated  $B$  (2023-1). The figure shows the  $\beta_{ik}$  coefficients obtained after running  $K = 27$  regressions of each  $k$  asset returns on the remaining  $K - 1$  asset returns for the period 2023-1. The vectors  $\beta_k$  are shown as rows of the matrix, and the diagonal elements are set equal to 1. The estimated matrix is non-symmetric (as  $\beta_{ik} \neq \beta_{ki}$ ), sparse (about 60% of the elements are equal to 0), and has only one element with a value greater than 1.

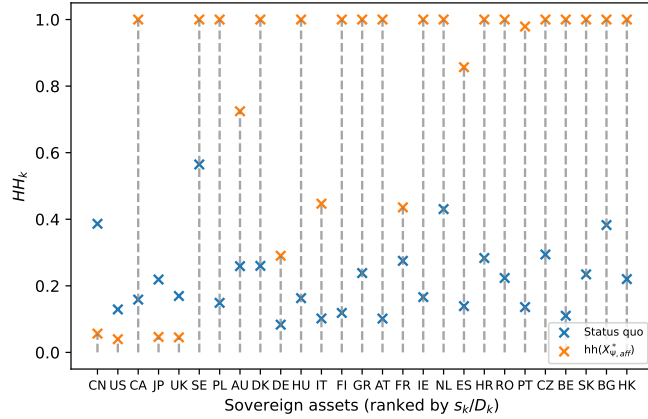


**Figure A.2:** Asset-level HH index by relative liquidity ( $s_k/D_k$ ) in  $\Psi^{aff}$ -optimum and status quo. We compare the asset-level Herfindahl-Hirschman index (which measures the degree to which assets are concentrated in banks' portfolios) for government assets. Assets are ranked by the ratio between the total outstanding volume available in the system  $s_k$  and the estimated market depth  $D_k$ , which measures the potential price impact of the asset in the system in the extreme case of a complete fire sale. The optimal structure shows a low degree of concentration, indicating higher diversification for larger and more liquid assets. In contrast, less liquid assets tend to be more concentrated, i.e. held by a smaller number of banks. This difference is particularly evident for larger assets such as Spanish, Italian, French and German government bonds. The optimal concentration for the first two assets is significantly higher than the status quo. German and French assets, on the other hand, are much more widely distributed across banks' portfolios. For larger assets, however, the possibilities for concentration are limited. This is because most banks cannot invest their portfolio in the entire outstanding amount of these assets. Portfolio concentration is thus determined by the interaction of size and liquidity.

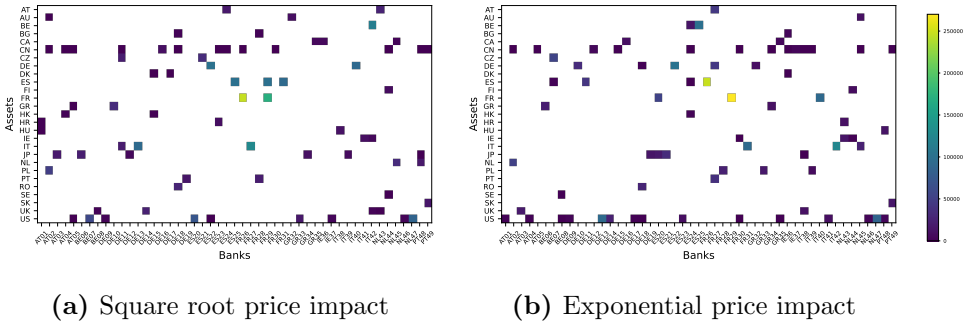


**Figure A.3:** Optimal solutions for alternative price impacts. Panel (a) shows the  $\Psi^{aff}$  optimal solution under the square root price impact ( $\mathbf{X}_{sqrt}^*$ ), while Panel (b) shows the  $\Psi^{aff}$  optimal solution under the exponential price impact ( $\mathbf{X}_{exp}^*$ ). Both systems have high degrees of concentration, higher than in the case of the linear specification (we observe an average HH index of 93.7 percent and 90.1 percent for the square root and exponential specifications, respectively).

**Table B.1:** Data sources.

ID	Country	Bond prices	Traded volumes	Public debt
AT	Austria	S&P All Maturities	Estimated	OECD
AU	Australia	S&P All Maturities	National	OECD
BE	Belgium	S&P All Maturities	National	OECD
BG	Bulgaria	Refinitiv 10Y	AFME	World Bank
CA	Canada	S&P All Maturities	National	OECD
CN	China	S&P All Maturities	asianbondsonline.org	World Bank
CZ	Czech Republic	S&P All Maturities	Estimated	OECD
DE	Germany	S&P All Maturities	National	OECD
DK	Denmark	S&P All Maturities	AFME	OECD
ES	Spain	S&P All Maturities	National	OECD
FI	Finland	S&P All Maturities	National	OECD
FR	France	S&P All Maturities	National	OECD
GR	Greece	S&P All Maturities	Estimated	OECD
HR	Croatia	Refinitiv 10Y	Estimated	World Bank
HK	Hong Kong	S&P All Maturities	National	World Bank
HU	Hungary	Refinitiv 10Y	AFME	OECD
IE	Ireland	S&P All Maturities	AFME	OECD
IT	Italy	S&P All Maturities	National	OECD
JP	Japan	S&P All Maturities	asianbondsonline.org	OECD
NL	Netherlands	S&P All Maturities	National	OECD
PL	Poland	S&P All Maturities	National	OECD
PT	Portugal	S&P All Maturities	National	OECD
TO	Romania	Refinitiv 10Y	National	National
SE	Sweden	S&P All Maturities	National	OECD
SK	Slovakia	Refinitiv 10Y	Estimated	OECD
UK	United Kingdom	S&P All Maturities	National	OECD
US	United States	S&P All Maturities	National	OECD

## B Sample data selection

We selected the sample as the largest list of banks-assets available for the period 2018-2023. The final sample includes 49 banks from 10 EMU countries and 27 country-specific sovereign assets. From the original list, we exclude all assets which are not referred to a specific country (i.e., exposures to generally identified regions), and sovereign assets for which no reliable data is available for the market. The data are collected at a semiannual periodicity, our final dataset comprising 11 semesters from 2018-Q2 to 2023-1. Information on counterparty country breakdown is available only for the total gross carrying amount of non-derivative financial assets, which is a total item including all instruments and maturities. For this reason, trading volumes data are collected for all-maturities instruments, and market price data refer to all-maturities instruments. A detailed list of sources is provided in Table B.1. For

some assets, trading volumes data are not publicly available, or just limited market segments are reported, potentially causing an underestimation of market liquidity for some instruments. In these cases, we used a simple regression approach to predict trading volumes using outstanding public debt, collected from various sources. Regressions for each year produce very high adjusted- $R^2$  coefficients (around 90% for all periods), thereby signalling the good predictive accuracy of outstanding public debt. The complete list of banks and the associated IDs used in the main part of the paper is provided in Table B.2.

**Table B.2:** List of selected banks.

Bank ID	Name	Bank ID	Name
AT01	BAWAG Group AG	FR26	BNP Paribas
AT02	Erste Group Bank AG	FR27	Groupe Cr�dit Agricole
AT03	Raiffeisen Bank International AG	FR28	Conf�d�ration Nationale du Cr�dit Mutuel
AT04	Raiffeisenbankengruppe O� Verbund eGen	FR29	Groupe BPCE
AT05	Volksbanken Verbund	FR30	RCI Banque
BE06	Belfius Bank	FR31	Soci�t� g�n�rale S.A.
BE07	KBC Groep	GR32	Alpha Services and Holdings S.A.
BE08	Investeringsmaatschappij Argenta	GR33	National Bank of Greece, S.A.
DE09	Aareal Bank AG	GR34	Piraeus Financial Holdings
DE10	Bayerische Landesbank	GR35	Eurobank Ergasias
DE11	Commerzbank AG	IE36	AIB Group plc
DE12	DekaBank Deutsche Girozentrale	IE37	Bank of Ireland Group plc
DE13	Deutsche Bank AG	IT38	Banca Popolare di Sondrio S.p.A.
DE14	DZ Bank AG	IT39	Credito Emiliano Holding S.p.A.
DE15	Hamburg Commercial Bank AG	IT40	Intesa Sanpaolo S.p.A.
DE16	Deutsche Pfandbriefbank AG	IT41	Mediobanca - Banca di Credito Finanziario S.p.A.
DE17	Erwerbsgesellschaft der S-Finanzgruppe mbH	IT42	Unicredit S.p.A.
DE18	Landesbank Hessen-Th�ringen	NL43	ABN AMRO Bank N.V.
DE19	Norddeutsche Landesbank	NL44	Co�peratieve Rabobank U.A.
ES20	Banco Bilbao Vizcaya Argentaria, S.A.	NL45	BNG Bank N.V.
ES21	Banco de Sabadell, S.A.	NL46	de Volksbank N.V.
ES22	Banco Santander, S.A.	NL47	ING Groep N.V.
ES23	Bankinter, S.A.	PT48	Banco Comercial Portugu�s, SA
ES24	Abanca Corporacion Bancaria, S.A.	PT49	Caixa Geral de Dep�sitos, SA
ES25	CaixaBank, S.A.		

## C Optimal solutions for a $2 \times 2$ system

We consider a financial system comprising 2 banks investing in 2 assets. Banks 1 and 2 have, respectively, total assets  $d_1$  and  $d_2$ , while assets 1 and 2 have outstanding amounts  $s_1$  and  $s_2$ . This system can be represented by the matrix:

$$\mathbf{X} = \begin{bmatrix} x_{11} & x_{12} \\ x_{21} & x_{22} \end{bmatrix}$$

Incorporating the constraints on banks' assets, we simplify the notation and formulate the system in terms of 2 variables:

$$x_{11} = x, \quad x_{12} = d_1 - x, \quad x_{21} = y, \quad x_{22} = d_2 - y$$

*Systemic Risk Minimization.* Given price impact parameters  $\gamma_1$  and  $\gamma_2$  for assets 1 and 2, the objective function for systemic risk minimization in the no-spillovers case is:

$$\Psi^{aff}(x, y) = \gamma_1 xy + \gamma_2(d_1 - x)(d_2 - y)$$

Thus, the optimization problem can be expressed as:

$$\begin{aligned} \min_{x,y} \quad & \Psi^{aff}(x, y) \\ \text{s.t.} \quad & x + y = s_1 \\ & x, y \geq 0 \end{aligned} \tag{C.1}$$

It is straightforward to prove that  $\Psi^{aff}(x, y)$  is strictly concave for all  $x$  and  $y$ . Due to concavity of the objective function, the solution to the minimization problem will be at one of the corners of the feasible set. In a perfectly symmetric system ( $d_1 = d_2$  and  $s_1 = s_2$ ), the minimum systemic risk solution will be either at  $x = 0, y = s_1$  or vice versa. Introducing asymmetry in the asset outstanding value distribution or in the banks' size distribution makes one of the maximum-concentration corners preferable, necessitating an evaluation of the objective function at each corner. While the minimum is located in one of the corners of the feasible set, the solutions to the first-order Kuhn-Tucker conditions identify a global maximum, which will be located at the point:

$$x^{max} = \frac{1}{2}s_1 + \left( \frac{\gamma_2}{\gamma_1 + \gamma_2} \right) (d_1 - d_2)$$

and

$$y^{max} = \frac{1}{2}s_1 + \left( \frac{\gamma_2}{\gamma_1 + \gamma_2} \right) (d_2 - d_1)$$

For perfectly symmetric systems where  $d_1 = d_2$ , the maximum systemic risk is reached at the perfect diversification portfolio, where each banks hold the same shares of the two assets. For asymmetric systems, e.g.,  $d_1 > d_2$ , the largest portfolio receives a larger share of the asset, proportional to its relative liquidity. Thus, maximum systemic risk portfolios are maximally diversified in homogeneous systems, while the optimization will tend to spread the less liquid asset across a larger number of portfolios, while concentrating more liquid assets, ceteris paribus. As we observed in Section 4, asset selection at the optima jointly depends on assets' price impact parameters and size, since the choice of which assets can be shared more in the system depends on the magnitude of the resulting portfolio overlaps.

*Individual Risk Minimization.* For the same  $2 \times 2$  system, the individual risk function, given the covariance matrix  $\Sigma$ , is expressed as:

$$\begin{aligned}\Upsilon(x, y) &= \sqrt{Ax^2 - 2d_1Bx + d_1^2\sigma_2^2} + \sqrt{Ay^2 - 2d_2By + d_2^2\sigma_2^2} \\ &= \sqrt{v_1(x)} + \sqrt{v_2(y)}\end{aligned}\tag{C.2}$$

where  $A = \sigma_1^2 + \sigma_2^2 - 2\sigma_{12}$  and  $B = \sigma_2^2 - \sigma_{12}$ , and  $v_1(x)$  and  $v_2(y)$  are, respectively, banks' 1 and 2 portfolio variances computed using asset holdings expressed in nominal terms  $x$  and  $y$ . From the minimization problem:

$$\begin{aligned}\min_{x,y} \quad & \Upsilon(x, y) \\ \text{s.t.} \quad & x + y = s_1 \\ & d_1 + d_2 = s_1 + s_2 \\ & x, y \geq 0\end{aligned}\tag{C.3}$$

we obtain the following first-order condition for interior solutions:

$$\frac{\partial \Upsilon(x^*, y^*)}{\partial x} = \frac{\partial \Upsilon(x^*, y^*)}{\partial y}$$

which, using (C.2), can be also expressed as:

$$\frac{dv_1(x^*)/dx}{dv_2(y^*)/dy} = \sqrt{\frac{v_1(x^*)}{v_2(y^*)}}\tag{C.4}$$

Since obtaining optimal values for  $x^*$  and  $y^*$  is analytically expensive, we adopt the following strategy. The maximum entropy (ME) values of  $x$  and  $y$  for a bipartite banks-asset system like ours are:

$$x^{\text{ME}} = \left(\frac{s_1}{s_1 + s_2}\right) d_1 \quad \text{and} \quad y^{\text{ME}} = \left(\frac{s_1}{s_1 + s_2}\right) d_2$$

If  $x^{\text{ME}}$  and  $y^{\text{ME}}$  respect the first-order conditions, then the ME structure is a solution to the minimization problem. We must verify that the following condition is satisfied:

$$\frac{dv_1(x^{\text{ME}})/dx}{dv_2(y^{\text{ME}})/dy} = \sqrt{\frac{v_1(x^{\text{ME}})}{v_2(y^{\text{ME}})}}$$

Replacing the expressions for  $x^{\text{ME}}$  and  $y^{\text{ME}}$ , we find that both the LHS and RHS of (C.4) simplify to  $d_1/d_2$ . While the RHS simplifies to  $d_1/d_2$  as well. Therefore,  $x^{\text{ME}}$  and  $y^{\text{ME}}$  are solutions for problem (C.3). One can also show that, for  $A > \frac{B}{d_1\sigma_2^2}$ ,  $\Upsilon(x, y)$  is strictly convex  $\forall x, y \in \mathbb{R}$ , and the ME structure is a unique solution to the minimization problem, which is the case for a wide range of parameter values.

## D Description of the optimization algorithm

When deterministic numerical optimization techniques cannot efficiently solve an optimization problem, non-deterministic heuristic methods can be useful alternatives (Gilli et al., 2019). This is true for the problem in (10), which consists of finding the matrix  $\mathbf{X}^*$  of bond holdings that minimizes individual and systemic risk as measured by some objective function, while ensuring that supply and demand of assets (marginal sums) are satisfied. For the problem at hand, we therefore propose a stochastic iterative method that can deal both with non-convex aspects in the objective functions as well as the constraints regarding networks. The basic functioning of the algorithm is described in the main text of the paper, while in this section we present the pseudocode both for the Evolutionary Search algorithm and for the mutation algorithm, respectively in Algorithms 1 and 2 below. The linear formulation we adopted for the price impact function also allows to express the problem as a quadratic program, which can be solved using standard quadratic programming tools. We did so in parallel experiments, to test the ability of the optimization algorithm to reach optimal solutions in simulated, smaller systems. In particular — besides using solvers readily available in R, Matlab, and Python — we implemented the quadratic-form systemic risk optimization in CPLEX and GUROBI, that provided consistent results, although with significantly longer execution times and non-converging procedures as the system becomes larger.

As for the technical implementation strategy, to avoid unwanted biases and premature convergence to local optima, non-deterministic optimization methods benefit from restarts with randomized initial solutions. To generate diverse yet feasible initial solutions, we employ two methods: one uses the status-quo network and performs the described mutation operation with a parameter  $p_m$  close to 1. Alternatively, an empty network is generated, and then, iteratively, a random element  $x_{ik}$  is picked and increased by a random amount  $0 < \delta \leq \min(d'_i, s'_k)$ , where  $d'_i$  and  $s'_k$  are the open demand of bank  $i$  and open supply of asset  $k$ , respectively, until all margins are allocated. In preliminary experiments, the algorithm was tested on artificial data sets for which the global optimum was known and was found to converge satisfactorily under suitable hyper-parameters. The hyper-parameters were then chosen based on experiments with the empirical data in this study. All reported results are based on at least 500 restarts per case, with typically one to five million function evaluations per restart. Therefore, reported results should be the global optima or at least very close. All implementations were done in Python 3.10, using the packages `numpy` and `multiprocessing` for numerical routines and parallelization, respectively.

---

**Algorithm 1:** EvoSearch( $\mathbf{X}$ ,  $f$ )

---

**Data:**  $\mathbf{X}$ : initial feasible network,  $f(\cdot)$ : objective function

**Result:**  $\mathbf{X}^* = \arg \min(f)$ , optimized feasible network that minimizes  $f$   
set population size  $PS$ , function evaluations  $FE$ , iterations  $T = FE/PS$

set parameters  $p_m$ ,  $\tau$ ,  $\Delta\tau = (\tau - 1)/T$

initialize  $\mathbf{X}_c = \text{mutate}(\mathbf{X}, 0.9)$ ,  $\mathbf{X}^* := \mathbf{X}_c$

**for**  $T$  iterations **do**

    generate mutants  $m = 1..PS$  with  $\mathbf{X}_m = \text{mutate}(\mathbf{X}_c, p_m)$

    identify best mutant:  $\mathbf{X}_e = \arg \min_m(f(\mathbf{X}_m))$

**if**  $f(\mathbf{X}_e) < f(\mathbf{X}_c) \cdot \tau$  **then**

        replace current solution:  $\mathbf{X}_c := \mathbf{X}_e$

**if**  $f(\mathbf{X}_e) < f(\mathbf{X}^*)$  **then**

            new acting optimum:  $\mathbf{X}^* := \mathbf{X}_e$

**return**  $\mathbf{X}^*$ 

---

---

**Algorithm 2:** mutate( $\mathbf{X}$ ,  $p_m$ )

---

**Data:**  $\mathbf{X}$ : network,  $p_m$ : controls amount of mutation

**Result:**  $\mathbf{Y}$ : mutated (= randomly modified) version of  $\mathbf{X}$

set probability to swap maximum amount  $p_f$

initialize new mutant,  $\mathbf{Y} := \mathbf{X}$

**repeat**

    pick two banks  $i \neq j$  and assets  $k \neq l$  such that  $y_{ik} > 0$ ,  $y_{jl} > 0$

    choose fraction to swap:  $\phi = 1$  with probability  $p_f$ ,  $0 < \phi < 1$  otherwise

    choose amount to swap:  $\Delta y = \phi \cdot \min(y_{ik}, y_{jl})$

    update bank  $i$ 's positions:  $y_{ik} := y_{ik} - \Delta y$ ,  $y_{il} := y_{il} + \Delta y$

    update bank  $j$ 's positions:  $y_{jk} := y_{jk} + \Delta y$ ,  $y_{jl} := y_{jl} - \Delta y$

**until**  $\text{rand} > p_m$  (exit loop with probability  $p_m$ );

**return**  $\mathbf{Y}$ 

---